European Journal of Operational Research 299 (2022) 1094–1110

Contents lists available at ScienceDirect

European Journal of Operational Research

journal homepage: www.elsevier.com/locate/ejor

Innovative Applications of O.R.

Risk-averse multi-stage stochastic optimization for surveillance and operations planning of a forest insect infestation

Sabah Bushaj[a], İ. Esra Büyüktahtakın[b,*], Robert G. Haight[c]

[a] State University of New York at Plattsburgh, NY, USA
[b] Systems Optimization and Data Analytics Lab (SODAL), Department of Mechanical and Industrial Engineering, New Jersey Institute of Technology, Newark, NJ, USA
[c] U.S. Department of Agriculture, Forest Service, Northern Research Station, St. Paul, MN USA

ARTICLE INFO

Article history:
Received 8 August 2020
Accepted 22 August 2021
Available online 3 September 2021

Keywords:
(R) OR in Natural Resources
Multi-Stage Stochastic Optimization
Risk-Averse
Conditional Value-at-Risk (CVaR)
Mixed Integer Programming
Scenario Dominance Cuts
Spatial-Temporal Optimization

ABSTRACT

We derive a nested risk measure for a maximization problem and implement it in a scenario-based formulation of a multi-stage stochastic mixed-integer programming problem. We apply the risk-averse formulation to the surveillance and control of a non-native forest insect, the emerald ash borer (EAB), a wood-boring beetle native to Asia and recently discovered in North America. Spreading across the eastern United States and Canada, EAB has killed millions of ash trees and cost homeowners and local governments billions of dollars. We present a mean-Conditional Value-at-Risk (CVaR), multi-stage, stochastic mixed-integer programming model to optimize a manager's decisions about surveillance and control of EAB. The objective is to maximize the benefits of healthy ash trees in forests and urban environments under a fixed budget. Combining the risk-neutral objective with a risk measure allows for a trade-off between the weighted expected benefits from ash trees and the expected risks associated with experiencing extremely damaging scenarios. We define scenario dominance cuts (sdc) for the maximization problem and under the decision-dependent uncertainty. We then solve the model using the sdc cutting plane algorithm for varying risk parameters. Computational results demonstrate that scenario dominance cuts significantly improve the solution performance relative to that of CPLEX. Our CVaR risk-averse approach also raises the objective value of the least-benefit scenarios compared to the risk-neutral model. Results show a shift in the optimal strategy from applying less expensive insecticide treatment to more costly tree removal as the manager becomes more risk-averse. We also find that risk-averse managers survey more often to reduce the risk of experiencing adverse outcomes.

1. Introduction

Multi-stage stochastic programming has been widely used in many fields, including but not limited to health-care (Yin & Büyüktahtakın, 2021a; 2021b), forestry (Kıbış et al., 2020), and finance (Abdelaziz, Aouni, & El Fayedh, 2007). Multi-stage stochastic programs typically minimize (maximize) an expectation criterion that calculates the expected cost (benefit) of all possible scenarios, each of which is mapped with a certain probability of occurrence. The expectation objective is useful in situations where the uncertainty does not indicate a potential for observing extreme events. However, if the environment features the possibility of experiencing high-impact events, even with small probabilities, the expectation criterion may not perform well because it does not capture the variability of events. In these situations, where a high impact scenario might happen, the expectation criterion is accompanied by a risk measure.

In this paper, we consider a risk-averse multi-stage stochastic mixed-integer program (RA-MSS-MIP), where the objective function is a combination of an expectation operator and a Conditional Value-at-Risk (CVaR) measure for each stage. We then apply this model to optimize the surveillance and control of a non-native forest insect, the emerald ash borer (EAB), which has infested large areas covered with ash trees in North America. The EAB is a wood-boring beetle native to Asia and discovered in the United States in 2002. Since its discovery, the EAB has killed millions of ash trees and cost homeowners and local governments billions of dollars.

EAB is a prime example of an invasive species - one that is transported outside of its native range and introduced to a non-native ecosystem causing economic or environmental harm. Effective management of invasive species has become a pressing problem because they threaten sustainability by adversely impacting the economy, the environment, and health. Invaders harm bio-

* Corresponding author.
E-mail address: esratoy@njit.edu (İ.E. Büyüktahtakın).

https://doi.org/10.1016/j.ejor.2021.08.035
0377-2217/

diversity and degrade the environment (Wilcove, Rothstein, Dubow, Phillips, & Losos, 1998); increase health problems by spreading many diseases (Juliano & Philip Lounibos, 2005), and affect food security by reducing the value of agricultural products (Pejchar & Mooney, 2009). Due to the substantial impacts on sustainability and human well-being, the international community, including the United Nations' Global Invasive Species Program (GISP), National Invasive Species Council (NISC), and Center for Invasive Species Management (CISM), has called for rapid control of invaders to minimize their adverse impacts (Büyüktahtakın & Haight, 2018).

This study addresses the problem of building a risk-averse spatial-dynamic model to help communities develop cost-effective strategies for the surveillance and control of EAB. Former multi-stage stochastic programming models of EAB surveillance and control decisions (Bushaj, Büyüktahtakın, Yemshanov, & Haight, 2021; Kıbış et al., 2020) only considered an expectation criterion in the objective function, the popular Risk Neutral measure. However, due to the intrinsic biological characteristics of the invader and some outside factors, such as careless transportation of infested wood, an infestation could spread fast, and substantial losses of ash trees could happen in a shorter time frame than expected. To alleviate the adverse impacts of experiencing such events, we consider a risk measure in the objective function in addition to the expectation criterion. The incorporation of the risk factors complicates the model, thus requiring advanced computational methodologies to solve it. To tackle the computational difficulty of the proposed complex risk-averse multi-stage stochastic mixed-integer program, we implement the scenario dominance cutting plane algorithm introduced in Büyüktahtakın (2021) to solve the RA-MSS-MIP model more efficiently. The effectiveness of these cuts is studied under the risk-neutral and risk-averse models. We provide insights on how risk-aversion affects decision-making, such as the budget allocated to insecticide treatment and tree removal. We also analyze the benefits of ash trees under risk compared to the original expectation criterion in the risk-neutral problem.

2. Literature review

2.1. Risk-averse stochastic programming

Traditional two-stage and multi-stage stochastic programs consider only expectation criterion in the objective function of the optimization problem based on the probability of each scenario, also known as a risk-neutral approach. In problems containing outliers in the distribution of the scenarios, the risk-neutral approach may perform poorly. Assuming that the manager wants to be careful of these extreme scenarios, in the risk-neutral approach, these undesirable outcomes associated with a bad scenario cannot be prevented. The solution obtained from optimizing the expected objective function will not consider the severe damages when one of these outlier scenarios happens. In such cases, risk-averse models become necessary. For example, in a disaster management situation (Escudero, Garín, Monge, & Unzueta, 2018a), non-repetitive decisions, such as facility locations (Escudero, Garín, & Unzueta, 2017), may result in a substantial operational cost or even an inability to fulfill the demand for a specific realization of the random parameters (Escudero, Monge, & Morales, 2018b).

One of the most popular risk measures is the VaR_α (Value-at-Risk), which represents the maximum possible loss over a time horizon at the confidence level α. While there has been much interest from academic researchers and industry, implementing the VaR is computationally challenging. In the last two decades, a new group of risk measures known as coherent risk measures is originated and studied extensively (Artzner, Delbaen, Eber, & Heath, 1997; Ogryczak & Ruszczyński, 1999). One of those coherent risk measures is the Conditional Value-at-Risk (CVaR), representing the weighted average of the extreme values in the tail of the distribution beyond the VaR cut-off. Rockafellar, Uryasev et al. (2000) present a technique on how to evaluate VAR and also optimize CVaR at the same time. It is shown that CVaR can be linearized and easily incorporated into a stochastic optimization problem, making it more preferable to VAR.

Mean-risk models, including VaR, have been widely used in financial optimization; however, the use of mean-risk models with CVaR in stochastic programming models is relatively new (Ahmed, 2006; Miller & Ruszczyński, 2011; Rockafellar et al., 2000; Schultz & Tiedemann, 2006). CVaR-based mean-risk stochastic programming has been studied in various applications, such as supply chain management (Alem & Morabito, 2013), reverse logistic network design (Soleimani & Govindan, 2014), and water resources planning (Alonso-Ayuso, Escudero, Guignard, & Weintraub, 2018; Zhang, Rahimian, & Bayraksan, 2016).

The majority of solution approaches presented for risk-averse multi-stage stochastic optimization problems are extensions of the solution techniques proposed for the risk-neutral equivalents Birge & Louveaux (2011). For example, Shapiro, Tekaya, da Costa, & Soares (2013) and Philpott & De Matos (2012) have extended the stochastic dual dynamic programming algorithm to risk-averse problems. Schultz & Tiedemann (2006) develop a Lagrangian decomposition algorithm to solve the scenario-based formulation of two-stage mixed-integer stochastic programming involving CVaR. Zhang et al. (2016) use a nested L-shaped method and investigated multiple cuts to improve the efficiency of a risk-averse multi-stage program. Guo & Ryan (2017) obtain lower bounds using the progressive hedging algorithm to solve time-consistent risk-averse multi-stage stochastic integer programs.

When formulating a risk-averse multi-stage stochastic problem, differently from mean-risk and two-stage stochastic problems, we have to be careful with time consistency. For risk-neutral and two-stage problems, consistency is ensured by default (Gollmer, Gotzes, & Schultz, 2011; Gollmer, Neise, & Schultz, 2008), but as stages increase, different methods to preserve time consistency are developed (Pflug & Pichler, 2016; Shapiro, 2012). Time consistency simply states that the decisions taken today must support the decisions that happened yesterday for the scenario that was realized. For example, following the time consistency definition in Alonso-Ayuso et al. (2018), let us assume that the decisions taken up to the realization of a group of scenarios, say scenario 1 to scenario n and stage $t' > 1$ (i.e., the decisions from stage 1 to stage $t'-1$ for this group of scenarios) have been made according to the solution obtained in the original model solved at stage $t = 1$. Then the rationale behind a time consistent risk-averse measure (RAM) is that the solution value to be obtained for any scenario in our group at time stage t' and the later solution values obtained in the scenario tree by the related submodel 'solved' at stage t' should have the same value as in the original model that is solved at stage $t = 1$. In other words, the scenarios that are not in the scenario group we select should not influence the solutions of the submodel at stage t' and later solutions for our scenario group (scenarios 1–n).

Pflug & Pichler (2016) have shown that measuring risk at each time stage separately and measuring the accumulation of risk over a scenario path are inconsistent. Ruszczyński & Shapiro (2006) propose a nested risk measure that proves to be consistent. They ensure its consistency by defining the appropriate conditional risk mappings in each stage, thus, presenting the risk formulation as a recursive function. Homem-de-Mello & Pagnoncelli (2016) propose a similar notion of a nested measure as Expected Conditional Risk Measure (ECRM). As the ECRMs consider only continuous variables, another type of risk measure that is increasingly used lately is also the Expected Conditional Stochastic Dominance (Escudero, Garín, Monge, & Unzueta, 2020; Escudero et al., 2018b), which is based on multi-stage stochastic dominance functional.

2.2. EAB control and risk-averse forest management planning

Invasive species pose a serious threat to the ecosystems they invade, and thus much research is performed to design surveillance and control strategies. Management of invasive species is a complex topic as each different invasive species has its specific behavior and biological characteristics. Many optimization problems are proposed for managing invasive species under a limited management budget (Albers, Fischer, & Sanchirico, 2010; Bushaj et al., 2021; Büyüktahtakin, Feng, Frisvold, & Szidarovszky, 2013; Büyüktahtakın, Feng, Frisvold, Szidarovszky, & Olsson, 2011; Hof, 1998; Huffaker, Bhat, & Lenhart, 1992; Kıbış & Büyüktahtakın, 2017; Kıbış et al., 2020; Kovacs, Haight, Mercader, & McCullough, 2014; Onal, Akhundov, Büyüktahtakın, Smith, & Houseman, 2020). For a detailed review of such optimization models, see, e.g., the reviews of Billionnet (2013) and Büyüktahtakın & Haight (2018).

EAB is one of the most damaging invasive species ever to reach the United States. Since its discovery in Michigan in 2002, EAB has spread to more than 37 U.S. states and five Canadian provinces, killing millions of ash trees and costing homeowners and local governments billions of dollars in damages (Aukema et al., 2011). To slow down the spread of EAB and reduce its harm, city, county, and state planners design surveillance and control strategies, usually with limited budgets. Kıbış et al. (2020) and Bushaj et al. (2021) addressed the cost-effective allocation of resources to survey and control of EAB. They integrate surveillance and control decisions and jointly optimize them to maximize the benefits of healthy ash trees by saving as many trees as possible. They model dispersal of EAB over time and space similar to discrete reaction-diffusion models (see, e.g., Büyüktahtakın, des Bordes, & Kıbış (2018); Kıbış & Büyüktahtakın (2019)) and surveillance to identify infested trees and their stage of infestation. Modeling EAB dispersal and ash tree health within the optimization model allows for targeted control decisions, such as insecticide treatment and tree removal, which are more cost-effective than naive decisions, such as removing all ash trees without ever surveying the severity of infestation.

The models of Kıbış et al. (2020) and Bushaj et al. (2021) considered only the expected maximum benefits of healthy ash trees in the objective function without emphasizing the risks and costs of low-chance, high-damage infestation scenarios. Optimal surveillance and control for EAB management may depend on the risk-aversion of managers, who seek to balance between maximizing the expected benefits of ash trees and minimizing the expected damage that could result under the worst possible scenarios of infestation growth.

While accounting for the risk-aversion of decision makers is standard in finance and economics, such accounting is limited in optimization models for forest management planning, including the surveillance and control of forest invasive species. Among the studies that use risk-averse management and stochastic optimization in forestry operations planning, Alonso-Ayuso et al. (2018) present a time-consistent mean-CVaR multi-stage programming model for planning the harvest of forest land designated for timber production and the construction of access roads needed to transport the timber. Pagnoncelli & Piazza (2017) present a stochastic dynamic programming model for harvest scheduling in which the decision maker wishes to minimize the overall CVaR of her decisions. On the other hand, Eyvindson & Cheng (2016) present a two-stage stochastic programming formulation with CVaR objectives to identify the optimal timing to measure and re-measure forest stands intending to maximize net present value. Yemshanov et al. (2019) use CVaR in a one-period model to develop optimal surveillance strategies that avoid worst-case outcomes of their surveying actions, where an outcome refers to the expected time to the first detection of a forest pest species.

2.3. Key contributions

The use of risk-averse stochastic programming is limited in forestry operations planning and invasive species management. Former risk-averse stochastic optimization approaches on invasive species control involved only a time domain of a single period. Our approach contributes to the OR and invasive species management literature in the following ways.

Modeling and Algorithmic Contributions. First, we derive a nested risk measure for a maximization problem and integrate it in a scenario-based formulation of a multi-stage stochastic programming problem to obtain a time-consistent formulation. Our time-consistent formulation is different than the node-based formulation of Alonso-Ayuso et al. (2018) in that we define the value-at-risk variable at each stage and under each scenario and include non-anticipativity constraints to impose that decisions and value-at-risk for those scenarios that share the same history up to a certain stage should be the same. Our definition of the risk-related constraints is similar to theirs in that we compute the positive difference between the value-at-risk at each stage and the total benefit up that time stage, and then penalize the expected difference in the objective function. Here, we focus on invasive species surveillance and control, while Alonso-Ayuso et al. (2018) study forest harvest management.

Second, we adapt the scenario dominance cutting planes introduced by Büyüktahtakın (2021) to the case of decision-dependent uncertainty. Specifically, we redefine the scenario dominance concept of Büyüktahtakın (2021) for our problem by considering the endogenous uncertainty modeled in our scenario tree and incorporated the surveillance pattern in defining the scenario dominance sets. We adapt the bounds and cuts to the problem with a maximization objective. Also, different than the method in Büyüktahtakın (2021), we provide a formal cutting plane algorithm, which systematically derives and adds cuts considering the decision-dependent uncertainty and specifics in our problem. While we apply those cuts to solve our case study problem, the proposed scenario dominance framework is general and can be applied to other mean-risk, multi-stage stochastic programming problems.

Third, we perform extensive computational analysis and present results regarding the optimal decision strategies under risk-averse and risk-neutral objectives. Our results demonstrate that scenario dominance cuts reduce the time complexity without an optimality gap. Furthermore, those cuts improve the initial integrality gap, and their performance is not affected by the changes in risk parameters.

Applied Contributions and Policy Insights. To our knowledge, we present the first risk-averse multi-stage stochastic programming model in the invasive species management literature. Multi-stage stochastic programming is superior to its two-stage counterparts because it can capture the spatial-dynamic features of the EAB infestation and its host trees over multiple time periods. Further, combining the risk-neutral objective with the risk measure allows managers to assess trade-offs between the weighted expectation objective and the risk of loss from low-probability, high-damage EAB scenarios. Using a CVaR risk-averse measure, we improve the benefit for the top $100 \times \alpha\%$ worst-case scenarios compared to the risk-neutral approach. Our model provides several important insights into the spatio-temporal dynamics and risk-averse management of EAB that would not be possible with existing models and methods, as summarized below:

- Our results suggest that, as the manager becomes more risk-averse, insecticide treatment becomes less preferred compared with tree removal, especially for scenarios that involve high infestation spread each year. This is an important practical finding

because forest managers often debate over two broad strategies for EAB management: surveillance and insecticide treatment of ash trees versus surveillance and staged removal of ash trees. Our results suggest that the former strategy may provide a higher expected net benefit while the latter strategy may provide a lower risk of outcomes with very low net benefits. The selection of the appropriate strategy will depend on the risk preference of the decision maker.
- Based on our results, increasing risk-aversion by emphasizing the poorly performing scenarios in the objective function might come at a price of reduced expected net benefit. Despite this price, the manager may see this loss as a worthy sacrifice towards the mitigation of possible disaster scenarios.
- Our analysis of surveillance frequency suggests that as we survey less, the expected risk increases due to higher uncertainty about infestation realizations. Thus, a risk-averse manager would want to survey more often.

In Section 3, we derive the risk measure for a maximization problem and present the general mean-risk multi-stage stochastic MIP framework. In Section 4, we describe notation and formulate the risk-averse multi-stage stochastic mixed-integer programming model for the EAB management in public forests. We derive the scenario dominance cuts and bounds presented in Büyüktahtakın (2021) for a maximization problem and present the associated theoretical results. Finally, in Section 6, we describe the implementation details of the model and test six different sets of data estimated by some prior knowledge of the EAB infestation in the state of New Jersey and provide computational results. We conclude the paper in Section 7.

3. Risk-averse MSS-MIP framework

3.1. General formulation of MSS-MIP

Let $\mathcal{T} = \{1, \dots, T\}$, where T represents the number of stages. Let n^t, h^t, q^t, and m^t represent the number of decision variables, the number of uncertain parameters, the number of integer variables, and the number of constraints, respectively, at time t. We denote the decisions to be taken at each stage $t = 1, \dots, T$ as $x^t \in \mathbb{R}_+^{n^t-q^t} \times \mathbb{Z}_+^{q^t}$ and the uncertainty observed in stage t as $\xi^t \in \mathbb{R}^{h^t}$, i.e., ξ^t is an $\mathcal{F}^t-$measurable mapping from Ω to $\mathbb{R}^{h^t}$.

The realization of ξ^{t+1} is known after the decision x^t in stage t. We denote the history of the realizations up to state t as $\xi^{[t]} = (\xi^1, \xi^2, \dots, \xi^t)$ for $t = 2, \dots, T$ and the decision history up to stage t as $x^{[t]} = (x^1, \dots, x^t)$ for $t = 1, \dots, T$, where ξ^1 is assumed to be known. In a t-stage model, the decision-realization sequence is formulated as $x^1, \xi^2, x^2(x^1, \xi^2), \xi^3, x^3(x^1, x^2, \xi^2, \xi^3), \dots, x^T(x^{[T]}, \xi^{[T]})$. The general formulation for a T-stage risk-neutral multi-stage stochastic mixed-integer program (MSS-MIP) is written as

$$\max \Big\{ f^1(x^1) + \mathbb{E}_{\xi^2}\Big[\max_{x^2} f^2(x^2, \xi^2) + \mathbb{E}_{\xi^3|\xi^{[2]}}\Big[\dots + \mathbb{E}_{\xi^T|\xi^{[T-1]}}\Big[\max_{x^T} f^T(x^T, \xi^T)\Big)\Big]\Big]\Big]\Big\} \tag{1}$$

subject to

$$A^1 x^1 \leq b^1 \tag{2}$$

$$A^t(\xi^{[t-1]})x^{t-1}(\xi^{[t-1]}) + W^t(\xi^{[t]})x^t(\xi^{[t]}) \leq b^t(\xi^{[t]}) \quad \forall\, t \in \mathcal{T} \setminus \{1\} \tag{3}$$

$$x^1 \in \mathbb{R}_+^{n^1-q^1} \times \mathbb{Z}_+^{q^1}; \quad x^t(\xi^{[t]}) \in \mathbb{R}_+^{n^t-q^t} \times \mathbb{Z}_+^{q^t} \quad \forall\, t \in \mathcal{T} \setminus \{1\}. \tag{4}$$

where $A^1 \in \mathbb{R}^{m^1 \times n^1}$ and $b^1 \in \mathbb{R}^{m^1}$ are known; and as time t progresses, the realization of uncertain parameter ξ^t is given by $A^t(\xi) \in \mathbb{R}^{m^t \times n^t}, W^t(\xi) \in \mathbb{R}^{m^t \times n^t}$, and $b^t(\xi) \in \mathbb{R}^{m^t}$; $f^t(x^t, \xi^t) : \mathbb{R}^{n^t \times h^t} \to \mathbb{R}$ represents a linear function for positive integers n^t and h^t such that $f^t(x^t, \xi^t) = c^t(\xi^t)x^t(\xi^t)$ where $c^t(\xi^t) \in \mathbb{R}_+^{n^t}$; and $\mathbb{E}_{\xi^t|\xi^{t-1}}[\cdot]$ is the expectation with respect to ξ^t depending on the random realization of the uncertainty, $\xi^{[t]}$.

3.2. CVaR, the risk averse measure of choice

Risk-neutral models simply consider the expected value of the objective function without any estimation of the variability of random outcomes. The expectation objective metric performs poorly under certain scenarios that have outliers with high variability. Depending on whether to maximize or minimize an objective function, one has to account for the large loss of profit or incurred costs falling in the tails of the objective value distribution. Next, we focus on and briefly discuss risk measures that are based on quantiles, such as the Value-at-Risk and the Conditional-Value-at-Risk, to mitigate large losses in the tails of the distribution of objective values.

Definition 3.1. Let $F_X(\cdot)$ represent the cumulative distribution function of a random variable X. The α-quantile of this distribution is called the Value-at-Risk (VaR). VaR is represented as:

$$\inf\{\eta \in \mathbb{R} : F_X(\eta) \geq 1 - \alpha\} \tag{5}$$

and denoted by $VaR_\alpha^+(X), \alpha \in (0, 1]$.

In a profit maximization context, VaR is the α-quantile of the distribution of the profits providing a lower bound on the distribution of profits, which is not fallen short of, with a defined probability $1 - \alpha$. For the profit maximization case, we use the values less than the threshold level of VaR to derive VaR_α^-. Because $VaR_\alpha^-(X) = VaR_\alpha^+(-X)$ the value-at-risk equation for a maximization problem becomes

$$VaR_\alpha^-(X) = -\sup\{\eta \in \mathbb{R} : F_X(\eta) \leq \alpha\}. \tag{6}$$

This representation still preserves the monotonicity, translation, and positive homogeneity properties of VaR (Artzner et al., 1997).

Definition 3.2. Conditional Value-at-Risk (CVaR) for a profit maximization function is defined as

$$CVaR_\alpha^-(X) = \mathbb{E}(X | X \geq VaR_\alpha^-(X)) \tag{7}$$

and represents the conditional expected shortage value, not reaching the value-at-risk at the confidence level α.

CVaR$^-$ for a random variable X at a confidence level α is formulated as (Rockafellar et al., 2000)

$$CVaR_\alpha^-(X) = \inf\left\{-\eta + \tfrac{1}{\alpha}\mathbb{E}(\eta - X)_+\right\} \tag{8}$$

where $(a)_+ = \max\{0, a\}$.

Despite the good properties it offers, the VaR is considered a non-coherent risk measure. The VaR also does not consider how bad the scenarios with an objective value below VaR_α^- can be. On the other hand, the CVaR is coherent and takes into account the scenarios in the α tail, thus, it is preferable to VaR (Acerbi & Tasche, 2002).

3.3. Time-consistent mean-risk MSS-MIP

The risk-neutral formulation (1)–(4) maximizes the expected value function without considering the impact of the extreme and unwanted scenarios on the expectation value. When the objective includes only expectation, the decision-maker will not mainly consider extreme loss scenarios, and a decision that works well for the

expectation may result in considerable costs in an extreme scenario. Combining the expected value formulation with risk measures enables the decision-maker to model a trade-off between the profit maximization on average and the risk minimization.

3.3.1. Deriving time-consistent CVaR

As mentioned above, there are different definitions of time consistency risk measures in literature; we refer to the definition provided in Homem-de-Mello & Pagnoncelli (2016). Let $(\Xi, \mathcal{F}, P)$ be a probability space and $\mathcal{F}^1 \subset \mathcal{F}^2 \subset \ldots \subset \mathcal{F}^T$ be sub sigma-algebras of $\mathcal{F}$. Let X^t denote a space of $\mathcal{F}^t$ -measurable function form Ξ to $\mathbb{R}$ and $X := X^1 \times X^2 \times \ldots \times X^T$. Then, a multi-stage risk function F is said to be a mapping from X to $\mathbb{R}$.

Homem-de-Mello & Pagnoncelli (2016) define the following multi-period risk function F as expected conditional risk measure (ECRM):

$$F(X^1, \ldots, X^T) = X^1 + \rho^2\left(X^2\right) + \mathbb{E}_{\xi^{[2]}}\left[\rho^3_{\xi^{[2]}}\left(X^3\right)\right] + \ldots + \mathbb{E}_{\xi^{[T-1]}}\left[\rho^T_{\xi^{[T-1]}}\left(X^T\right)\right], \quad (9)$$

where $\rho^t_{[\xi^t]}$ represents the risk measure at time t. Homem-de-Mello & Pagnoncelli (2016) prove that any risk function F defined as in (9) is time consistent, provided that each $\rho^t_{[\xi^t]}$ satisfies some basic properties that automatically hold, for example, for coherent risk measures.

Using the "tower property" of expectations, F defined in (9) could be re-written as:

$$F(X^1, \ldots, X^T) = X^1 + \rho^2\left(X^2\right) + \mathbb{E}_{\xi^{[2]}}\left[\rho^3_{\xi^{[2]}}\left(X^3\right) + \mathbb{E}_{\xi^{[3]}}\left[\rho^4_{\xi^{[3]}}\left(X^4\right) + \ldots + \mathbb{E}_{\xi^{[T-1]}}\left[\rho^T_{\xi^{[T-1]}}\left(X^T\right)\right]\ldots\right]\right]. \quad (10)$$

Homem-de-Mello & Pagnoncelli (2016) consider the conditional value at risk of the realization at time t as a particular case of ECRMs defined in (9) and (10). That is $\rho^t_{[\xi^t]} = CVaR^{[\xi^t]}_{\alpha^t}$, where

$$CVaR^{[\xi^t]}_{\alpha^t} = \max_{\eta^t \in \mathbb{R}} \eta^t - \frac{1}{\alpha^t}\mathbb{E}_{\xi^{[t]}}\left[\left(\eta^t - f^t\left(x^t, \xi^t\right)\right)_+ | \xi^{[t-1]}\right]. \quad (11)$$

Using $CVaR^{[\xi^t]}_{\alpha^t}$ as our risk measure in (10), we can formulate our 5-stage time-consistent $\mathbb{E} - CVaR$ model as below:

$$\begin{aligned}\max_{x^1,\ldots,x_T} \quad & f^1(x^1) + \max_{\eta^2 \in \mathbb{R}} \ \eta^2 - \frac{1}{\alpha^2}\mathbb{E}_{\xi^{[2]}}\left[(\eta^2 - f^2(x^2, \xi^2))_+\right] \\ & + \mathbb{E}_{\xi^{[2]}}\left[\max_{\eta^3 \in \mathbb{R}} \ \eta^3 - \frac{1}{\alpha^3}\mathbb{E}_{\xi^{[3]}}\left[(\eta^3 - f^3(x^3, \xi^3))_+ | \xi^{[2]}\right]\right] \\ & + \mathbb{E}_{\xi^{[3]}}\left[\max_{\eta^4 \in \mathbb{R}} \ \eta^4 - \frac{1}{\alpha^4}\mathbb{E}_{\xi^{[4]}}\left[(\eta^4 - f^4(x^4, \xi^4))_+ | \xi^{[3]}\right]\right] \\ & + \mathbb{E}_{\xi^{[4]}}\left[\max_{\eta^5 \in \mathbb{R}} \ \eta^5 - \frac{1}{\alpha^5}\mathbb{E}_{\xi^{[5]}}\left[(\eta^5 - f^5(x^5, \xi^5)) \right.\right. \\ & \left.\left. + \ | \xi^{[4]}\right] | \xi^{[4]}\right] | \xi^{[3]}\right] | \xi^{[2]}\Big] \end{aligned} \quad (12)$$

subject to

$$x^t \in X^t(X^{[t-1]}, \xi^{[t]}) \quad \forall\ t = 2, 3, \ldots, T.$$

where X^t represents the decisions up to stage $t-1$ considering the realization of uncertainty parameter up to stage t ($\xi^{[t]}$).

If the uncertain process is discretized by considering a finite number of realizations of ξ, each random realization over time is named as a scenario, and its index is denoted by ω. Let Ω be the set of scenarios. Each scenario $\omega \in \Omega$ has a corresponding probability p_ω of occurring. Each decision denoted as $x^t_\omega := x^t\left(\xi^t_\omega\right)$, represents the decision for the scenario realization up to stage t, ξ^t_ω, for $t = 1, \ldots, T$. Defining a new variable v^t_ω to account for the positive difference between η^t_ω and x^t_ω for each $t \in \mathcal{T}$, we linearize formulation (12) by imposing two additional constraints for each time stage t:

$$v^t_\omega \geq 0 \qquad \text{and} \qquad v^t_\omega \geq \eta^t_\omega - \sum_{t'=1}^{t} f^{t'}(x^{t'}_\omega, \xi^{t'}_\omega) \qquad \forall\ t = 2, \ldots, T. \quad (13)$$

For each stage t, the auxiliary variable η^t_ω is a "stage-$(t-1)$ variable," representing the value-at-risk, $VaR^{[\xi^t]}_{\alpha^t}$. We use an auxiliary variable v^t_ω, which is a "stage-t variable," to represent the stage-t shortage value, not reaching η^t_ω.

The general $\mathbb{E} - CVaR$ optimization problem can be formulated as a dynamic program, which then can be cast into a scenario-based formulation (see Online Supplement Section S2).

3.3.2. Mean-risk scenario-based MSS-MIP formulation

The CVaR takes into account the benefit for those unwanted scenarios that are below the VaR. However, it does not consider scenarios with a higher benefit than the VaR, which are also included in the expectation objective function. On the other hand, the objective function with only a risk measure, without considering the profit, will provide non-efficient solutions. Consequently, the decision maker prefers a trade-off between risk minimization and benefit maximization. Therefore, in the presence of uncertainty, a widely used approach among practitioners and researchers is to combine the risk measures with the optimization of the expected value of the objective function, leading to the mean-risk models introduced by Markowitz (1952) (see, e.g., Alonso-Ayuso et al. (2018); Ogryczak & Ruszczyński (2001); Schultz & Tiedemann (2006)). Using the $CVaR^-_\alpha$ in Equation (8) as a risk measure, we consider the following mean-risk problem within a maximization context:

$$\max_{x \in \mathcal{X}} \left\{\mathbb{E}(f(x_\omega, \xi_\omega)) + \lambda CVaR^-_\alpha(f(x_\omega, \xi_\omega))\right\}, \quad (14)$$

where λ represents a trade-off coefficient between the expected benefit and the loss due to risk, and $\mathcal{X}$ represents the set of feasible solutions for x. In the mean-risk formulation (14), the manager can easily shift from risk-neutral to risk-averse by adjusting the λ parameter. Setting λ to 0, the expression (14) would be equivalent to the expectation objective (no matter what α value is). Additionally, giving a certain weight to λ and using α to decide on the size of the tail of the objective value distribution enables the manager not only to decide on the risky values but also to determine how important they are with respect to the expectation.

Using the linearization shown in (13), we present the $\mathbb{E} - CVaR$ optimization problem as a general risk-averse multi-stage stochastic mixed-integer program (RA-MSS-MIP) below:

$$P: \max_{\substack{x^1,\ldots,x^T \\ \eta^2,\ldots,\eta^T \\ v^1,\ldots,v^T}} \sum_{\omega \in \Omega} p_\omega \left(\sum_{t=1}^{T} c^t_\omega x^t_\omega + \lambda \sum_{t=2}^{T}\left(\eta^t_\omega - \frac{1}{\alpha^t} v^t_\omega\right)\right) \quad (15)$$

subject to

$$v^t_\omega \geq \eta^t_\omega - \sum_{t'=1}^{t} c^{t'}_\omega x^{t'}_\omega \qquad \forall\ \omega \in \Omega,\ t \in \mathcal{T} \setminus \{1\}, \quad (16)$$

$$A^1 x^1_\omega \leq b^1_\omega \qquad \forall\ \omega \in \Omega, \quad (17)$$

$$A^t_\omega x^{t-1}_\omega + W^t_\omega x^t_\omega \leq b^t_\omega \qquad \forall\ \omega \in \Omega,\ t \in \mathcal{T} \setminus \{1\}, \quad (18)$$

$$x^t_\omega \in \mathbb{R}_+^{n^t - q^t} \times \mathbb{Z}_+^{q^t} \qquad \forall \omega \in \Omega,\ t \in \mathcal{T}, \quad (19)$$

$$v_\omega^t \geq 0 \qquad \forall \omega \in \Omega,\ t \in \mathcal{T}, \tag{20}$$

$$x_\omega^t = x_{\omega'}^t\ v_\omega^t = \quad v_{\omega'}^t \qquad \forall\ t \in \mathcal{T};\ \omega, \omega' \in \Omega\ s.t.\ \xi_\omega^{[t]} = \xi_{\omega'}^{[t]}. \tag{21}$$

where the random parameters are realized as $\xi_\omega^t = \left(c_\omega^t, b_\omega^t, A_\omega^t, W_\omega^t\right)$ for each $t \in \mathcal{T}$ and $\omega \in \Omega$.

An important constraint in the scenario-based representation of the RA-MSS-MIP problem in maximization formulation (15)-(21) is Equation (21). The non-anticipativity Equation (21) implies that decisions for all scenarios that share the same history up to a specific time t are the same and ensures the implementability of solutions (Rockafellar & Wets, 1991; Wets, 1974). It also implies that the decision chosen at time t may only depend on the realizations of ξ up to that time period and not on the results of future observations. Furthermore, enforcing non-anticipativity constraints on v_ω^t plays a crucial role in ensuring the time-consistency of the multi-stage decisions.

4. RA-MSS-MIP for the surveillance and operations planning of EAB

We apply the mean-CVaR formulation (15)-(21) to optimize the surveillance and control of the EAB, which has infested large areas covered with ash trees in North America. This section presents the notation and the RA-MSS-MIP formulation for the surveillance, treatment, and removal planning of the ash trees for the EAB infestation. We also provide a verbal description of the model and the assumptions made as well as an example multi-stage scenario tree in the Online Supplement Section S1.

4.1. Notation

Sets and Indices

Γ Set of all sites, $\Gamma = \left\{1, 2, \ldots, \bar{\Gamma}\right\}$.
K Set of infestation levels, $K = \{1, 2, 3\}$.
$\mathcal{T}$ Set of time periods, $\mathcal{T} = \{1, \ldots, T\}$.
χ Set of neighboring layers that a spread can happen from a site i; each layer represents a distance-dependent neighbor of site i with similar spread rates.
Ω Set of scenarios in a scenario tree, $\Omega = \left\{1, \ldots, \bar{\Omega}\right\}$.
i Index for site where $i \in \Gamma$.
Θ_i^ι Set of neighboring sites of site i at layer ι.
k Index for infestation level where $k \in K$.
t Index for time period where $t \in \mathcal{T}$.
j Index for neighboring sites of site i at layer ι where $j \in \Theta_i^\iota$.
ω Index for a scenario where $\omega \in \Omega$.
ι Index for neighboring layer where $\iota \in \chi$.

Parameters

p_ω Probability for scenario ω.
c_1 Cost of surveying (inspecting) a tree.
c_2 Cost of treatment.
c_3 Cost of removal.
ζ Monetary value of a susceptible tree.
ϑ_k Penalty value of each infested tree at infestation level k.
r_k Impact rate of each infested tree at infestation level k within site i, i.e., number of new infestations per infested tree at level k.
ϱ Surveillance efficiency, i.e., percent of infested trees that are identified correctly.
τ Discount rate.
δ_t Discount factor at time t, which is equal to $\frac{1}{(1+\tau)^t}$.
Ψ Total budget available.
θ_k^ι Infestation impact of k^{th}-level infested trees in neighboring layer ι belonging to site j.
κ Maximum number of trees surveyed in each site i.
γ_i Number of surveyed trees in site i under surveillance at time t,i.e., $\gamma_i = \min\left(N_{i\omega}^t, \kappa\right)$.
$p_{j\to i}^\iota$ Probability of infestation spread from site j to i at neighboring layer ι.
$\beta_{k\omega}^t$ Percentage change in belief of infestation after surveillance for infestation level k, at time t, for scenario ω.
$\bar{N}_i$ Initial number of tree population at site i.
$\bar{I}_{ik}$ Initial number of infested tree population at each infestation level k, at site i.

Decision Variables

$N_{i\omega}^t$ Total number of trees at site i, at time t, for scenario ω
$S_{i\omega}^t$ Number of susceptible trees at site i, at time t, for scenario ω
$\widetilde{I}_{ik\omega}^t$ Believed number of infested trees at site i, at time t, for infestation level k, for scenario ω before surveillance
$\ddot{I}_{ik\omega}^t$ Transition number of infested trees at site i, at time t, at infestation level k, for scenario ω after surveillance without considering total tree population
$I_{ik\omega}^t$ Estimated number of infested trees at site i, at time t, at infestation level k, for scenario ω after surveillance with considering total tree population
$V_{ik\omega}^t$ Number of treated trees at site i, at time t, at infestation level k, for scenario ω
$R_{ik\omega}^t$ Number of removed trees at site i, at time t, at infestation level k, for scenario ω
$H_{i\omega}^t$ Number of trees surveyed at site i, at time t for scenario ω
$Q_{ik\omega}^t$ Number of infested trees remaining after treatment and removal at site i, at time t, at infestation level k, for scenario ω

Risk Variables

η_ω^t value-at-risk parameter
v_ω^t Linearization variable for the risk constraint

Binary Decision Parameters in Decision Scenario Tree

$$y_\omega^t = \begin{cases} 1 & \text{if surveillance is applied at time } t, \text{for scenario } \omega \\ 0 & \text{otherwise} \end{cases}$$

Linearization Variables

$$u_{ik\omega}^t = \begin{cases} 1 & \text{if transition population is assigned to infestation} \\ & \text{level } k, \text{at site } i \text{ at time } t \\ 0 & \text{otherwise} \end{cases}$$

4.2. Mathematical model

Following the convention in Bushaj et al. (2021), we present the following RA-MSS-MIP formulation for the surveillance and control of the EAB as follows:

$$Max \sum_{\omega\in\Omega} p_\omega \left(\sum_{t\in\mathcal{T}} \left(\delta_t \sum_{i\in\Gamma} \left(\zeta S_{i\omega}^t - \sum_{k=1}^{n} \vartheta_k I_{ik\omega}^t \right) \right) + \lambda \sum_{t=2}^{T} \left(\eta_\omega^t - \frac{1}{\alpha} v_\omega^t \right) \right) \tag{22}$$

Subject to :

Risk Linearization Constraint

$$v_\omega^t \geq \quad \eta_\omega^t - \sum_{t'=2}^{t} \delta_{t'} \sum_{i\in\Gamma} \left(\zeta S_{i\omega}^{t'} - \sum_{k=1}^{n} \vartheta_k I_{ik\omega}^{t'} \right) \quad \forall\ \omega \in \Omega,\ t \in \mathcal{T} \setminus \{1\}, \tag{23}$$

Initial Total Population

$$N_{i\omega}^1 = \bar{N}_i \qquad \forall\ \omega,\ i, \tag{24}$$

Initial Belief of Infestation

$$\widetilde{I}_{ik\omega}^1 = \bar{I}_{ik} \qquad \forall\ \omega,\ i,\ k, \tag{25}$$

Population Constraint

$$N_{i\omega}^{t+1} = N_{i\omega}^{t} - \sum_{k=1}^{n-2} V_{ik\omega}^{t} - \sum_{k=1}^{n} R_{ik\omega}^{t} \qquad \forall\ \omega,\ i,\quad t = 1, \tag{26}$$

$$N_{i\omega}^{t+1} = N_{i\omega}^{t} - \sum_{k=1}^{n-2} V_{ik\omega}^{t} - \sum_{k=1}^{n} R_{ik\omega}^{t} + \sum_{k=1}^{n-2} V_{ik\omega}^{t-1} \quad \forall\ \omega,\ i,\ t = 2 \ldots T-1, \tag{27}$$

Transition Infestation Level

$$\ddot{I}_{ik\omega}^{t} = \tilde{I}_{ik\omega}^{t}\left(1 + x_{\omega}^{t}\beta_{k\omega}^{t}\right) \qquad \forall\ \omega,\ i,\ t,\ k, \tag{28}$$

Number of Treated and Removed Trees

$$V_{ik\omega}^{t} + R_{ik\omega}^{t} \le I_{ik\omega}^{t} \sum_{a=max[t-k+1,1]}^{t} y_{\omega}^{a} \qquad \forall\ \omega,\ i,\ t,\quad k = 1, \tag{29}$$

$$R_{ik\omega}^{t} \le I_{ik\omega}^{t} \sum_{a=max[t-k+1,1]}^{t} y_{\omega}^{a} \qquad \forall\ \omega,\ i,\ t,\quad k = n-1,\ n, \tag{30}$$

Susceptible (Healthy) Tree Population

$$S_{i\omega}^{t} = N_{i\omega}^{t} - \sum_{k=1}^{n} I_{ik\omega}^{t} \qquad \forall\ \omega,\ i,\ t, \tag{31}$$

Carrying Capacity Constraints

$$I_{ik\omega}^{t} \le N_{i\omega}^{t} - \sum_{d=min(k+1,n)}^{n} I_{id\omega}^{t} \qquad \forall\ \omega,\ i,\ t,\ k, \tag{32}$$

$$I_{ik\omega}^{t} \le \ddot{I}_{ik\omega}^{t} \qquad \forall\ \omega,\ i,\ t,\ k, \tag{33}$$

$$\ddot{I}_{ik\omega}^{t} - I_{ik\omega}^{t} \le \bar{N}_{i}\left(1 - u_{ik\omega}^{t}\right) \qquad \forall\ \omega,\ i,\ t,\ k, \tag{34}$$

$$\left(N_{i\omega}^{t} - \sum_{d=min(k+1,n)}^{n} I_{id\omega}^{t}\right) - I_{ik\omega}^{t} \le \bar{N}_{i} u_{ik\omega}^{t} \qquad \forall\ \omega,\ i,\ t,\ k, \tag{35}$$

Believed (Expected) Number of Infested Trees

$$\tilde{I}_{i1\omega}^{t+1} = \sum_{k=1}^{n} Q_{ik\omega}^{t\iota} r_{k} + \sum_{k=1}^{n} \sum_{\iota \in \chi} \sum_{j \in \Theta_{i}^{\iota}} Q_{jk\omega}^{t\iota} \theta_{k}^{\iota} p_{j\to i}^{\iota} \quad \forall \omega,\ i,\ \iota,\ j,\ t = 1 \ldots T-1, \tag{36}$$

$$Q_{ik\omega}^{t\iota} = \begin{cases} I_{ik\omega}^{t\iota} - \varrho V_{ik\omega}^{t\iota} - \varrho R_{ik\omega}^{t\iota} & k = 1 \\ I_{ik\omega}^{t\iota} - \varrho R_{ik\omega}^{t\iota} & k = n-1\ \ n \end{cases} \qquad \forall\ \omega,\ i,\ t,\ \iota, \tag{37}$$

$$\tilde{I}_{ik\omega}^{t+1} = I_{i(k-1)\omega}^{t} - \varrho V_{i(k-1)\omega}^{t} - \varrho R_{i(k-1)\omega}^{t} \quad \forall\ \omega,\ i,\ t = 1 \ldots T-1,\ k = 2, \tag{38}$$

$$\tilde{I}_{ik\omega}^{t+1} = \left(I_{i(k-1)\omega}^{t} - \varrho R_{i(k-1)\omega}^{t}\right) + \left(I_{ik\omega}^{t} - \varrho R_{ik\omega}^{t}\right) \qquad \forall\ \omega,\ i,\ t = 1 \ldots T-1,\ k = n, \tag{39}$$

Budget Constraint

$$c_{1} \sum_{t\in\mathcal{T}} \sum_{i\in\Gamma} H_{i\omega}^{t} + c_{2} \sum_{t\in\mathcal{T}} \sum_{i\in\Gamma} \sum_{k=1}^{n-2} V_{ik\omega}^{t} + c_{3} \sum_{t\in\mathcal{T}} \sum_{i\in\Gamma} \sum_{k=1}^{n} R_{ik\omega}^{t} \le \Psi \qquad \forall\ \omega,\ i,\ t,\ k, \tag{40}$$

$$H_{i\omega}^{t} = \gamma_{i} x_{\omega}^{t} \qquad \forall\ \omega,\ i,\ k,\ t = 1, 2, \ldots, T, \tag{41}$$

$$\gamma_{i} = \min\left(N_{i\omega}^{t}, \kappa\right) \quad \forall\ \omega,\ i,\ t, \tag{42}$$

Non-anticipativity Constraints

$$\begin{array}{llll} N_{i\omega}^{t} = N_{i\omega'}^{t} & S_{i\omega}^{t} = S_{i\omega'}^{t} & \tilde{I}_{ik\omega}^{t} = \tilde{I}_{ik\omega'}^{t} & \\ I_{ik\omega}^{t} = I_{ik\omega'}^{t} & \ddot{I}_{ik\omega}^{t} = \ddot{I}_{ik\omega'}^{t} & V_{ik\omega}^{t} = V_{ik\omega'}^{t} & \forall\ \omega = \omega' \in \Omega\ s.t.\ \xi_{\omega}^{[t]} = \xi_{\omega'}^{[t]},\ \forall\ i,\ t,\ k, \\ \eta_{\omega}^{t} = \eta_{\omega'}^{t} & v_{ik\omega}^{t} = v_{ik\omega'}^{t} & R_{ik\omega}^{t} = R_{ik\omega'}^{t} & \end{array} \tag{43}$$

Non-negativity and Binary Restrictions

$$N_{i\omega}^{t},\ S_{i\omega}^{t},\ I_{ik\omega}^{t},\ \tilde{I}_{ik\omega}^{t},\ \ddot{I}_{ik\omega}^{t},\ V_{ik\omega}^{t},\ R_{ik\omega}^{t} \ge 0 \quad u_{ik\omega}^{t} \in \{0,1\} \qquad \forall\ \omega,\ i,\ k. \tag{44}$$

The objective function of our model given in (22) is a mean-risk scenario formulation of the form shown in function (15). Here, the expectation part represents the total value of the health trees, which we call as the expected profit, while the risk part refers to the expected profit of the risky scenarios that exceeds a threshold value, *VaR*. The λ allows the manager to adjust the level of risk-averseness between the expectation and the risk. As the λ value is increased, the decision-maker becomes more risk-averse by putting a higher weight on the bad scenarios that could occur. Constraint (23) represents the linearization of the risk parameter.

In constraints (24) and (25), we define the initial value of the tree population and the expected initial infestation levels for each site i and for all possible scenarios $\omega \in \Omega$ for the initial time period 1. Constraints (26) and (27) keep track of the current population based on decisions made for removing and treating trees.

Constraint (28) computes the believed infestation level for each k. Depending on the surveillance regime and the realization value β, for each infestation level k, the believed number of infested trees in each site i is calculated.

Constraints (29) and (30) serve as a limit on how many trees can be treated and removed, respectively. The total number of treated and removed trees cannot be more than the number of infested trees. Furthermore, if no surveillance is performed for several periods in a row, then no treatment or removal can be applied.

Constraint (31) keeps track of the number of susceptible trees for each site i by deducting every infested tree from the total population. Constraints (32)–(35) are used as the linearization of the carrying capacity constraint, which is a non-linear equation given below:

$$I_{k\omega}^{t} = \min\left(N_{i\omega}^{t} - \sum_{d=min(k+1,n)}^{n} I_{id\omega}^{t},\ \ddot{I}_{ik\omega}^{t}\right) \tag{45}$$

Constraint (45) states that as infestation continues, there is a limit on how many trees can get infested and how many trees can die. In the worst case, if no management decision is taken at all, this limit is constrained by the total number of trees in each site i.

Constraints (32) and (33) serve as an upper bound on the number of estimated infested trees, while constraints(34) and (35) serve as a lower bound by using an auxiliary binary decision variable $u_{ik\omega}^{t}$.

Constraints (36) - (39) define the number of newly infested trees for each infestation level k for the time period $t+1$. When trees are neither treated nor removed in infestation level k, they are passed to the next infestation level $k+1$ in the next period. Once trees reach the last infestation level $k = n$, if not removed, they still stay in that same infestation level. Constraints (36) - (39) represent the growth of infestation over time and space, similar to discrete reaction-diffusion models (see, e.g., Büyüktahtakın et al. (2018); Holmes, Lewis, Banks, & Veit (1994); Kıbış & Büyüktahtakın (2019)).

Constraint (36) estimates the number of trees that will be in infestation level $k = 1$. This is done by collectively calculating the effect of infested trees on susceptible trees nearby. The term $p_{j\to i}^{\iota}$ in constraint (36) defines the probability that infestation will spread from site j to site i located at the ι^{th} distance class from j. When calculating dispersal, we cover a radius of 4-km from the infested site. We handle these distance classes using the term θ_{i}^{ι} in constraint (36). The unremoved or untreated trees in each of these sites are denoted by the term $Q_{ik\omega}^{t\iota}$ as given in constraint (37).

Constraint (40) ensures that the cost of surveillance, treatment, and removal is under the budget available throughout the planning horizon. Constraint (43) ensures that scenarios with the same history up to a given stage t share the same decisions until that stage, also known as non-anticipativity constraints in the scenario formulation. Finally, constraint (44) defines the non-negativity con-

straints on the decision variables and defines the linearization variable $u^t_{ik\omega}$, as a binary variable. For a more detailed description of the risk-neutral version of the mathematical model above, we refer the reader to the explanation in Bushaj et al. (2021).

5. Scenario dominance decomposition

In this section, we present the scenario dominance concept, the scenario sub-problem, the bounds obtained from the scenario sub-problem, and the scenario dominance cuts introduced by Büyüktahtakın (2021) for RA-MSS-MIPs. We first provide those definitions and results for the general risk-averse maximization problem (P) (15)-(21), and then show the adaptation of these concepts to derive the dominance relations, bounds, and cuts to improve the solvability of our case-study problem (22) – (44), which involves decision-dependent uncertainty.

Definition 5.1 The scenario-ω problem Büyüktahtakın, 2021
The scenario-ω problem P_ω is formulated as follows:

$$Z_\omega = \max\, p_\omega \left(\sum_{t=1}^{T} c^t_\omega x^t_\omega + \lambda \sum_{t=2}^{T} \left(\eta^t_\omega - \frac{1}{\alpha^t} v^t_\omega \right) \right) \tag{46}$$

s.t. Constraints (16) to (21).

Remark 1 The scenario-ω problem (46) is an MIP, which includes all the variables and the constraints of the original problem P. However, having an objective defined only for a single scenario ω improves the solution time compared to the original problem (15)-(21), P.

Definition 5.2 The relaxed scenario- ω problem
The relaxed scenario- ω problem P^R_ω is defined as follows:

$$Z^R_\omega = \max\, p_\omega \left(\sum_{t=1}^{T} c^t_\omega x^t_\omega + \lambda \sum_{t=2}^{T} \left(\eta^t_\omega - \frac{1}{\alpha^t} v^t_\omega \right) \right) \tag{47}$$

s.t. Constraints (16) to (20). Note that P^R_ω is obtained by removing the non-anticipativity constraints (21) in P_ω.

Definition 5.3 The classical scenario-ω problem
The classical scenario-ω problem P^C_ω is defined as follows:

$$Z^C_\omega = \max\, p_\omega \left(\sum_{t=1}^{T} c^t_\omega x^t_\omega + \lambda \sum_{t=2}^{T} \left(\eta^t_\omega - \frac{1}{\alpha^t} v^t_\omega \right) \right) \tag{48}$$

s.t. Constraints (16) to (20) pertaining only to scenario-ω problem. Note that P^C_ω is obtained by reducing the solution space to that of only scenario-ω.

Proposition 1. *P^R_ω is a relaxation of P_ω:*

$$Z^R_\omega \geq Z_\omega \quad \forall\ \omega \in \Omega. \tag{49}$$

Proof. It is easy to see that the feasible region of P_ω is a subset of the feasible region of P^R_ω. That is $\mathcal{X} \subseteq \mathcal{X}^{\mathcal{R}}$, where $\mathcal{X}$ is the feasible region of the original problem, P, and $\mathcal{X}^{\mathcal{R}}$ is the feasible set of solutions for the relaxed scenario-ω problem, P^R_ω. □

P^C_ω is obtained by removing constraints (21) from P and decomposing the model to $|\Omega|$ independent sub-models, each of them related to one scenario ω. On the other hand, P^R_ω includes all the constraints and variables of the original problem except the constraints (21). Because P^C_ω and P^R_ω are not defined in the same space, P^C_ω is not a relaxation of P^R_ω. Yet, the optimal objective value of P^C_ω provides an upper bound on the optimal objective value of P^R_ω, as shown in Proposition 2 below.

Proposition 2.

$$Z^C_\omega \geq Z^R_\omega \quad \forall\ \omega \in \Omega. \tag{50}$$

Proof. Let $(\ddot{x}_\omega, \ddot{\eta}_\omega, \ddot{v}_\omega)$ be the optimal solution for the scenario-ω problem, P^R_ω. Substituting this solution into the objective function of the problem P^C_ω, we have:

$$Z^C_\omega \geq p_\omega \left(\sum_{t=1}^{T} c^t_\omega \ddot{x}^t_\omega + \lambda \sum_{t=2}^{T} \left(\ddot{\eta}^t_\omega - \frac{1}{\alpha^t} \ddot{v}^t_\omega \right) \right) = Z^R_\omega. \tag{51}$$

□

Remark 2. From Propositions 1 and 2, it is easy to see that:

$$Z^C_\omega \geq Z^R_\omega \geq Z_\omega \quad \forall\ \omega \in \Omega. \tag{52}$$

5.1. Sub-additivity and upper bound

Let x^* be the optimal solution for the original problem (15)-(21) (P), and $Z(x^*)$ be the corresponding objective function value. Let $\dot{x}_\omega$ be the optimal solution for scenario-ω problem P_ω and $Z_\omega(\dot{x}^\omega)$ be the corresponding optimal objective value. Also, let $\bar{x}_\omega$ be the optimal solution to the classical scenario-ω problem P^C_ω and $Z^C_\omega(\bar{x}_\omega)$ be the corresponding objective function value.

Next, we provide the classical definition of a sub-additive set function.

Definition 5.4. Let Ω be a set and $\phi : 2^\Omega \to \mathbb{R}$ be a set function, where 2^Ω denotes the power set. The function ϕ is sub-additive if $\forall\ a, b \subset \Omega$, we have $\phi(a) + \phi(b) \geq \phi(a \cup b)$.

Definition 5.5Multiple Scenario Problem. Let $\bar{\Omega} \subseteq \Omega$. Then the multiple scenario problem including the set $\bar{\Omega}$, $P_{\bar{\Omega}}$ is formulated as below:

$$Z_{\bar{\Omega}} = \max \sum_{\omega \in \bar{\Omega}} p_\omega \left(\sum_{t=1}^{T} c^t_\omega x^t_\omega + \lambda \sum_{t=2}^{T} \left(\eta^t_\omega - \frac{1}{\alpha^t} v^t_\omega \right) \right) \tag{53}$$

s.t. Constraints (16) to (21).

Proposition 3. *$Z_{\bar{\Omega}}$ is subadditive on $\bar{\Omega} \subset \Omega$, which means that for $\Omega_1, \Omega_2 \subset \Omega$*

$$Z_{\Omega_1} + Z_{\Omega_2} \geq Z_{\Omega_1 \cup \Omega_2}. \tag{54}$$

Proof. Consider P_{Ω_1}, P_{Ω_2} and $P_{\Omega_1 \cup \Omega_2}$. All those three problems share the same feasible region with P. Thus, using the optimal solution of the $P_{\Omega_1 \cup \Omega_2}$, a feasible but sub-optimal solution can be built for each of P_{Ω_1} and P_{Ω_2}. □

Remark 3. Using a similar proof in Proposition 3, it is easy to see that the inequality (54) also holds for the classical scenario-ω problem P^C_ω, whose feasible set is only limited to that of only scenario-ω.

Proposition 4. *(**Upper Bound**) $\sum_{\omega \in \Omega} Z_\omega$ provides an upper bound on the optimal objective function value of the original problem, i.e.,*

$$\sum_{\omega \in \Omega} Z_\omega \geq Z(x^*). \tag{55}$$

Proof. The proof follows from the generalization of the sub-additivity property in Proposition 3 to include all scenarios $\omega \in \Omega$. □

5.2. Lower bound

Let $\dot{x}_\omega$ be the optimal solution for the scenario-ω problem P_ω and $Z(\dot{x}_\omega)$ be the objective value of the original problem P where $\dot{x}_\omega$ is substituted in the original problem objective function.

Remark 4. $Z(\dot{x}_\omega)$ is a lower bound on the objective function value of the original problem as follows:

$$Z(x^*) \geq Z(\dot{x}_\omega) \ \forall \ \omega \ \in \ \Omega. \tag{56}$$

As inequality (56) holds for each $\omega \in \Omega$, $Z(x^*)$ is bounded below by the maximum of $Z(\dot{x}_\omega)$ over all $\omega \in \Omega$, i.e.,

$$Z(x^*) \geq max_{\omega \in \Omega} \ Z(\dot{x}_\omega). \tag{57}$$

5.3. Scenario dominance

As described in Section 3.1, we define scenario ξ_ω as the realization path of a random variable ξ over multiple time stages $t \in \mathcal{T}$. Therefore, we derive scenario dominance relations by comparing the realizations of the uncertainty parameter ξ at each time stage t for two different scenarios. Below we first give the original definition of the scenario dominance concept for the general RA-MSS-MIP introduced by Büyüktahtakın (2021) and then provide the definition of scenario dominance for our case-study problem (22) – (44) presented in Section 4.

Definition 5.6 Scenario Dominance. (Büyüktahtakın, 2021). Considering a scenario realization at time $t \in \mathcal{T}$ as $\xi^t_\omega := (c^t_\omega, b^t_\omega, A^t_\omega, W^t_\omega)$ and two specific scenarios ξ_a and ξ_b, scenario ξ_a dominates scenario ξ_b, denoted by $\xi_b \preceq \xi_a$, for the original problem (15)–(21) (P) if

$$(p_a \geq p_b) \ \wedge \ (c^t_a \geq c^t_b) \ \wedge \ (b^t_a \geq b^t_b) \ \wedge \ (A^t_a \leq A^t_b) \\ \wedge \ (W^t_a \leq W^t_b) \ \forall \ t \in \mathcal{T}, a, b \in \Omega$$

and the scenario-ω problem objective function $p_\omega\left(\sum_{t=1}^T c^t_\omega x^t_\omega + \lambda \sum_{t=2}^T \left(\eta^t_\omega - \frac{1}{\alpha^t} v^t_\omega\right)\right)$ is a non-decreasing function for $\omega = a, b \in \Omega$.

Here we define the scenario dominance relations and sets for the EAB surveillance and operations planning problem presented in Section 4. We provide a detailed verbal description of the model in the Online Supplement Section S1. An example scenario tree is demonstrated in Figure S1, and its description is also provided in the Online Supplement Section S1.1 for this problem. This scenario tree depicts the sequences of possible surveillance decisions and the stochastic infestation outcomes over time. Here, there are three outcomes of infestation depending on the surveillance action: low (L) or high (H) if surveillance is performed and medium (M) if surveillance is not performed. Then, L-L-L-M-H represents a specific scenario for a 5-stage problem, where a low realization is observed for the first three years after surveying trees each year, followed by a medium realization without any surveillance, and a high realization at the last stage of the planning horizon after the surveillance is performed.

Here, a dominating scenario is a scenario in which the uncertainty realization at each period is lower, thus providing a higher objective compared to some other scenario. Since our objective is the maximization of the benefits of healthy ash trees, a scenario having a lower EAB infestation provides a higher objective than the one with a higher infestation. For example, defining a scenario having a low (L) infestation realization over five years in consecutive as *L-L-L-L-L* and a scenario with a high (H) infestation realization over the next five years by *H-H-H-H-H*, the scenario *L-L-L-L-L* dominates the scenario *H-H-H-H-H* if also its probability is larger than the scenario *H-H-H-H-H* because it leads to less infested trees in each time period.

Similar to the study of Büyüktahtakın (2021), a scenario dominates another scenario if only it yields a higher objective function value. Specific to our problem, we take management action only when we apply surveillance. When we compare two scenarios, we need to consider the surveillance regime of each. For the two scenarios with a different surveillance regime, we cannot be sure which would be the dominating one. We modify the scenario dominance concept defined in Büyüktahtakın (2021) to our problem described in Section 4 and present the following definition.

Definition 5.7. In our case-study problem, in addition to the probability of a scenario ω, p_ω, and the left-hand side uncertainty parameter, $\beta^t_{k\omega}$, which represents the percentage change in belief of infestation after surveillance for infestation level k, time t, and scenario ω (see constraint (28)), we also consider the surveillance regime. Therefore, considering our scenario realization at $t \in \mathcal{T}$ as $\xi^t_\omega := \beta^t_{k\omega}$ for $\omega \in \Omega$ and $k \in K$, and given two scenario realizations ξ_a and ξ_b that share the same surveillance regime, scenario ξ_a dominates scenario ξ_b, denoted as $\xi_b \preceq \xi_a$, for the case-study problem (22) – (44), if

$$(p_a \geq p_b) \ \wedge \ (\beta^t_{ka} \leq \beta^t_{kb}) \quad \forall \ t \in \mathcal{T}, \quad k \in K, \ a, b \in \Omega.$$

Based on Definitions 5.6 and 5.7, we now present the dominance set.

Definition 5.8 Dominance Set. The set of scenarios which are dominated by scenario $\xi_a \in \Omega \quad (\Lambda^+_{(\xi_a)})$ are described below:

$$\Lambda^+_{(\xi_a)} = \{b \in \Omega : \xi_b \preceq \xi_a\}.$$

5.4. Cuts based on scenario dominance

In this section, we first present the main results and scenario dominance cuts for solving the general risk-averse multi-stage stochastic mixed-integer programs. The theoretical results are mainly adapted from Büyüktahtakın (2021). Different than Büyüktahtakın (2021) we focus on RA-MSS-MIP with a maximization objective and decision dependent uncertainty. Thus, we specify the cuts for our case-study problem and further present a formal cutting plane algorithm, which systematically generates and adds cuts considering the decision-dependent uncertainty.

Definition 5.9. Let $x^*_\omega := (x^*_\omega, \eta^*_\omega, v^*_\omega)$ be the portion of the optimal solution of the original problem that corresponds to scenario ξ_ω and $\bar{Z}(x^*_\omega)$ be the portion of the objective function value at x^*_ω, such that:

$$\bar{Z}(x^*_\omega) = p_\omega\left(\sum_{t=1}^T c^t_\omega x^{t*}_\omega + \lambda \sum_{t=2}^T \left(\eta^{t*}_\omega - \frac{1}{\alpha^t} v^{t*}_\omega\right)\right). \tag{58}$$

Definition 5.10. Let $\dot{x}_\omega := (\dot{x}_\omega, \dot{\eta}^t_\omega, \dot{v}^t_\omega)$ be the optimal solution for the scenario ξ_ω problem P_ω and $Z_\omega(\dot{x}_\omega)$ be the corresponding optimal objective function value such that:

$$Z_\omega(\dot{x}_\omega) = p_\omega\left(\sum_{t=1}^T c^t_\omega \dot{x}^t_\omega + \lambda \sum_{t=2}^T \left(\dot{\eta}^t_\omega - \frac{1}{\alpha^t} \dot{v}^t_\omega\right)\right). \tag{59}$$

Lemma 1. *The optimal objective value of scenario ξ_a problem P_a, $Z_a(\dot{x}_a)$, and the objective value portion of the original problem corresponding to scenario ξ_a, $\bar{Z}(x^*_a)$, are related in the following way:*

$$\bar{Z}(x^*_a) \leq Z_a(\dot{x}_a) \ \forall \ a \in \ \Omega. \tag{60}$$

Proof. Assume that for some $a \in \Omega$ we have:

$$Z_a(\dot{x}_a) < \bar{Z}(x^*_a).$$

Then, we define a new solution to the scenario-ξ_a as below:

$$\ddot{x}^t_a = x^{t*} \ \forall \ t \in \ \mathcal{T}. \tag{61}$$

This new solution $\ddot{x}^t_a$ is feasible since x^* is optimal to the original problem and increases the value of $Z_a(\dot{x}_a)$, which contradicts the optimality of $\dot{x}_a$ for the scenario-ξ_a problem. □

Lemma 2. *Let ξ_a and ξ_b be two scenarios such that $\xi_a \preceq \xi_b$. Let $\dot{x}_a$ and $\dot{x}_b$ be the optimal solution of scenario ξ_a and ξ_b problems, respectively. Then, the optimal objective value of the scenario ξ_a, $Z_a(\dot{x}_a)$, and*

the optimal objective value of the scenario ξ_b, $Z_b(\ddot{x}_b)$, have the following relation:

$$Z_a(\dot{x}_a) \leq Z_b(\ddot{x}_b) \qquad \forall\ a \in \Lambda^+_{(\xi_b)}. \tag{62}$$

Proof. Let $\tilde{P}_b$ and $\tilde{P}_a$ be two new problems by adding the following inequalities to both scenario-ω problems, in this case, P_b and P_a, respectively:

$$x^t_b = x^t_a \ \forall\ t\ \in \mathcal{T}. \tag{63}$$

We define the following two sets as below:

$$\Omega' = \Big(\omega \in \Omega \setminus \{\{a\},\{b\}\} : \exists\ t \in \mathcal{T}\ \textit{such that}\ \ \xi^{[t]}_\omega = \xi^{[t]}_a\ \ \textit{for some}\ t > 1\Big).$$

$$\Omega'' = \Big(\omega \in \Omega \setminus \big\{\Omega' \cup \{a\} \cup \{b\}\big\}\Big).$$

Then, we say that $\Omega = \Omega' \cup \Omega'' \cup \{a\} \cup \{b\}$. Note that the set Ω' only includes scenarios $\omega \neq \{a, b\}$ that share a common history with scenario a up to stage t. Therefore, Ω'' is not an empty set, and $\Omega = \Omega' \cup \Omega'' \cup \{a\} \cup \{b\}$. Let $\tilde{x}$ be a feasible solution for both problems, $\tilde{P}_b$ and $\tilde{P}_a$, as below:

$$\tilde{x}^t_b = \ddot{x}^t_b$$

$$\tilde{x}^t_a = \ddot{x}^t_b$$

$$\tilde{x}^t_\omega = \ddot{x}_{\dot{\omega}}\ \forall\ \omega \in \Omega',\ \dot{\omega} \in \Omega$$
$$s.t.\ \xi^{[t]}_\omega = \xi^{[t]}_a \quad \textit{for}\ t = 1,\ldots,t'$$
$$\xi^{[t]}_{\dot{\omega}} = \xi^{[t]}_b \quad \textit{for}\ t = 1,\ldots,t'$$
$$\xi^{[t]}_\omega = \xi^{[t]}_{\dot{\omega}} \quad \textit{for}\ t = t'+1,\ldots,t$$

$$\tilde{x}^t_\omega = \ddot{x}^t_\omega \quad \forall\ \omega \in \Omega''.$$

The solution defined above is feasible for both of the problems, $\tilde{P}_a$ and $\tilde{P}_b$ because it satisfies all the constraint of the original problem, including the non-anticipativity constraints. We define the optimal objective function values of the problems $\tilde{P}_a$ and $\tilde{P}_b$ as $\tilde{Z}_a$ and $\tilde{Z}_b$, respectively. The solution of $\tilde{x}$ for $\tilde{P}_b$ because for each feasible solution x_b, we have $\tilde{Z}_b(x_b) \geq Z_b(x_b)$ and $\tilde{Z}_b(\tilde{x}) = Z_b(\tilde{x}) = Z_b(\ddot{x}_b)$. Due to no uncertainty in the objective, the decisive parameters are the probability of each scenario to happen p_ω and the uncertainty in left-hand side $\beta^t_{k\omega}$. Because $p_b > p_a$ and $\beta^t_{kb} \leq \beta^t_{ka}$ and a feasible solution vector $\tilde{x}_a$ has to satisfy constraints related to scenario ξ_b due to equation (63), we get

$$\tilde{Z}_b(\tilde{x}) \geq \tilde{Z}_a(\tilde{x}) \tag{64}$$

$$\tilde{Z}_a(\tilde{x}_a) \geq Z_a(\dot{x}_a). \tag{65}$$

Because $\tilde{x} = \ddot{x}_b$, we have

$$\tilde{Z}_b(\tilde{x}) = Z_b(\ddot{x}_b). \tag{66}$$

Furthermore, we can say that

$$Z_b(\ddot{x}_b) = \tilde{Z}_b(\tilde{x}) \geq \tilde{Z}_a(\tilde{x}) \geq Z_a(\dot{x}_a). \tag{67}$$

□

Theorem 1. *Let ξ_a and ξ_b be two scenarios such that $\xi_a \preceq \xi_b$, where $a,\ b\ \in \Omega$ and $a \neq b$. Then, the optimal objective value corresponding to scenario-ξ_b problem, $Z_b(\ddot{x}_b)$, and the objective value portion of the original problem for scenario ξ_a, $\bar{Z}(x^*_a)$, have the following relation:*

$$\bar{Z}(x^*_a) \leq Z_b(\ddot{x}_b) \qquad \forall\ a \in \Lambda^+_{(\xi_b)}, \tag{68}$$

where

$$\bar{Z}(x^*_a) = p_a\left(\sum_{t=1}^{T} c^t_a x^{t\,*}_a + \lambda \sum_{t=2}^{T}\left(\eta^{t\,*}_a - \frac{1}{\alpha^t}\upsilon^{t\,*}_a\right)\right). \tag{69}$$

Proof. From Lemma 1, we have $\bar{Z}(x^*_a) \leq Z_a(\dot{x}_a)$, and from Lemma 2, we have $Z_a(\dot{x}_a) \leq Z_b(\ddot{x}_b)$. Therefore, we can state that:

$$\bar{Z}(x^*_a) \leq Z_a(\dot{x}_a) \leq Z_b(\ddot{x}_b),$$

where $\ddot{x}_b$ is the optimal solution to the scenario-ξ_b problem. □

Remark 5 Trade-off between bound and time. Although scenario-ω formulation P_ω with all the constraints of the original problem provides a better bound than P^C_ω, depending on the size of the problem, P^C_ω could be faster to solve compared to P_ω. Since P^C_ω provides an upper bound on P_ω, the inequality (68) in Theorem 1 can be adapted to the following inequality (***sdc***):

$$\bar{Z}(x^*_a) \leq Z^C_b(\vec{x}_b) \qquad \forall\ a \in \Lambda^+_{(\xi_b)}, \tag{70}$$

where $\vec{x}_b$ is the optimal solution for P^C_b.

Proposition 5 Strong Scenario Dominance Cuts (ssdc). *Let ξ_b be a scenario with $b \in \Omega$, and $\ddot{x}^t_b$ represent the partial optimal solution to the scenario-ξ_b problem and $x^{t\,*}_a$ represent the partial optimal solution corresponding to scenario ξ_a, where $a \in \Omega$, in the original problem P, such that $\xi_a \preceq \xi_b$ holds for each time period 1 to t. Then the optimal objective value corresponding to scenario-ξ_b problem over time periods 1 to t, $Z^t_b(\ddot{x}^t_b)$ and the objective value of the original problem for scenario-ξ_a over time periods 1 to t, $\bar{Z}^t(x^{t\,*}_a)$ have the following relation:*

$$\bar{Z}^t\left(x^{t\,*}_a\right) \leq Z^t_b\left(\ddot{x}^t_b\right) \quad \forall\ a \in \Lambda^+_{\xi_b,t},\ \forall\ t\ \in\ \mathcal{T}, \tag{71}$$

where $\Lambda^+_{\xi_b,t}$ represents the set of scenarios that are dominated by scenario ξ_b for time periods 1 to t and

$$\bar{Z}^t\left(x^{t\,*}_a\right) = p_a\left\{\sum_{j=1}^{t} c^j_a x^{j\,*}_a + \lambda \sum_{j=2}^{t}\left(\eta^{j\,*}_a - \frac{1}{\alpha^j}\upsilon^{j\,*}_a\right)\right\}. \tag{72}$$

Remark 6 Adapting sdc to the case-study problem. The **sdc** (70) given in Remark 5 can be adapted to our case-study problem (22) – (44) by defining $\bar{Z}(x^*_\omega)$ and $Z^C_\omega(\vec{x}_\omega)$, respectively, as follows:

$$\bar{Z}(x^*_\omega) = p_\omega\left(\sum_{t\in\mathcal{T}}\left(\delta_t \sum_{i\in\Gamma}\left(\zeta S^{t*}_{i\omega} - \sum_{k=1}^{n}\vartheta_k I^{t*}_{ik\omega}\right)\right) + \lambda\sum_{t=2}^{T}\left(\eta^{t*}_\omega - \frac{1}{\alpha}\upsilon^{t*}_\omega\right)\right), \tag{73}$$

$$Z^C_\omega(\vec{x}_\omega) = p_\omega\left(\sum_{t\in\mathcal{T}}\left(\delta_t \sum_{i\in\Gamma}\left(\zeta \vec{S}^t_{i\omega} - \sum_{k=1}^{n}\vartheta_k \vec{I}^t_{ik\omega}\right)\right) + \lambda\sum_{t=2}^{T}\left(\vec{\eta}^t_\omega - \frac{1}{\alpha}\vec{\upsilon}^t_\omega\right)\right). \tag{74}$$

Remark 7 Adapting ssdc to the case-study problem. The **ssdc** (71) given in Proposition 5 can be adapted to our case-study problem (22) – (44) by defining $\bar{Z}^t\left(x^{t*}_\omega\right)$ and $Z^t_\omega(\ddot{x}_\omega)$, respectively, as follows:

$$\bar{Z}^t\left(x^{t*}_\omega\right) = p_\omega\left(\sum_{j=1}^{t}\left(\delta_j \sum_{i\in\Gamma}\left(\zeta S^{j*}_{i\omega} - \sum_{k=1}^{n}\vartheta_k I^{j*}_{ik\omega}\right)\right) + \lambda\sum_{j=2}^{t}\left(\eta^{j*}_\omega - \frac{1}{\alpha}\upsilon^{j*}_\omega\right)\right), \tag{75}$$

$$Z^t_\omega(\ddot{x}^t_\omega) = p_\omega\left(\sum_{j=1}^{t}\left(\delta_j \sum_{i\in\Gamma}\left(\zeta \ddot{S}^j_{i\omega} - \sum_{k=1}^{n}\vartheta_k \ddot{I}^j_{ik\omega}\right)\right) + \lambda\sum_{j=2}^{t}\left(\ddot{\eta}^j_\omega - \frac{1}{\alpha}\ddot{\upsilon}^j_\omega\right)\right). \tag{76}$$

Remark 8. In the case of **sdc**, we compare two scenario realizations based on their respective probabilities (p_ω), left-hand side uncertainty parameter ($\beta^t_{k\omega}$), and the surveillance regime. For strong scenario dominance cuts (**ssdc**), we value each of these conditions for up to a time period t. Depending on specific applications, **ssdc** might even cut the optimal solution. In our problem, by involving the surveillance regime in the dominance definition, we prevent these cuts from cutting off the optimal solution.

5.4.1. Cutting-plane algorithms

We formally describe the steps of the scenario dominance cutting plane (sdc) algorithm under Algorithm 1a and the strong scenario dominance cutting plane (ssdc) algorithm under Algorithm 1b. Initially, we formulate the scenario sub-problems. Studying the relation between scenarios and the uncertainty realized after the surveillance, we can define and formulate the dominance relations. In dominance sets, we specify how each scenario relates to another. This part is crucial to decide which cuts are used. For scenario dominance, we group scenarios in five categories considering how many periods in total we surveyed. Using the dominance relations, we can now create dominance sets. Depending on the number of scenarios, a problem may have many cuts. Once solving the randomly selected scenario sub-problem, we use dominated scenarios in set Λ_{ω}^{+} to define the scenario dominance cuts.

To generate the strong scenario dominance cuts, we care that the surveillance perfectly matches in periods from 1 to t for two scenarios compared in the cut. Defining a scenario up to each time t as $\omega^{[t]}$, we define a set of scenarios that are dominated by scenario $\omega^{[t]}$ and denote this set as $\Phi_{\omega^{[t]}}^{+[t]}$. Then, we select the best scenario to solve the sub-problem and add cuts for all the dominated scenarios in set $\Phi_{\omega^{[t]}}^{+[t]}$.

Algorithm 1 Algorithms for sdc (1a) and ssdc (1b)

(a) Scenario Dominance Cut Generation

Procedure: Define Dominance Sets
Define: β_{ω}, p_{ω}, Λ_{ω}^{+}, Λ_{ω}^{-}, N_{ω}
for $\omega \in \Omega$ **do**
  for $\omega' \in \Omega$ **do**
    if ω and ω' have same number of surveyed periods **then**
      if $\beta_{\omega} \leq \beta_{\omega'}$ and $p_{\omega} \geq p_{\omega'}$ **then**
        append ω' **to** Λ_{ω}^{+}
        append ω **to** $\Lambda_{\omega'}^{-}$
      else
        append ω **to** $N_{\omega'}$
        append ω' **to** N_{ω}
      end if
    end if
  end for
end for

Procedure: Create Cut Map
Define: Υ, n {Υ : *set of scenarios used as upper bound in the cut; n : cardinality of* Υ}
Define: *map* $\langle \omega \in \Upsilon, \Lambda_{s}^{+} \rangle$ {*Mapping a scenario to the scenarios dominated by it*}
for $i \in [0, n]$ **do**
  select a random scenario $\omega^{r} \in \Lambda_{\omega^{r}}^{+}$
  add the pair { $\omega^{r} : \Lambda_{\omega^{r}}^{+}$ } to map
end for

Procedure: Add Scenario Dominance Cut
Solve P_{ω} and obtain Z_{ω}
Define $x_{\omega^{r}}$ {$x_{\omega^{r}}$: *decision variables corresponding to scenario* ω^{r}}
Define $\bar{Z}(x_{\omega^{r}})$ {$\bar{Z}(x_{\omega^{r}})$: *objective value portion of the original problem for scenario* ω^{r}}
Define cutNum {*cutNum : the number of cuts added* $\forall \omega \in \Upsilon$}
for $i \in [0, cutNum]$ **do**
  select scenario $\omega^{r} \in \Lambda_{s}^{+}$
  add cut: $Z_{\omega} \geq \bar{Z}(x_{\omega^{r}})$
end for

(b) Strong Scenario Dominance Cut Generation

Procedure: Define Strong Dominance Sets
Define: $\omega^{[t]}$ {$\omega^{[t]}$: *scenario* ω *from time 1 to t*}
Define: $\beta_{\omega^{[t]}}$ {$\beta_{\omega^{[t]}}$: *uncertainty realization of scenario* ω *from time 1 to t*}
Define: $p_{\omega^{[t]}}$ {$p_{\omega^{[t]}}$: *probability of scenario* ω *from time 1 to t*}
Define: $\Phi_{\omega^{[t]}}^{+[t]}$ {$\Phi_{\omega^{[t]}}^{+[t]}$: *set of scenarios dominated by scenario* ω *from time 1 to t*}
for $t \in \mathcal{T}$ **do**
  for $\omega^{[t]} \in \Omega$ **and** $\omega'^{[t]} \in \Omega$ **do**
    if $\omega^{[t]}$ and $\omega'^{[t]}$ have the same surveyed periods from time 1 to t **then**
      if $\beta_{\omega}^{[t]} \leq \beta_{\omega'^{[t]}}$ and $p_{\omega^{[t]}} \geq p_{\omega'^{[t]}}$ **then**
        append $\omega'^{[t]}$ **to** $\Phi_{\omega^{[t]}}^{+[t]}$
      end if
    end if
  end for
end for

Procedure: Add Strong Scenario Dominance Cut
Solve $P_{\omega^{[t]}}$ and obtain $Z_{\omega^{[t]}}^{[t]}$ {$P_{\omega^{[t]}}$: *sub-problem for scenario* $\omega^{[t]}$, $Z_{\omega^{[t]}}^{[t]}$: *objective value of* $P_{\omega^{[t]}}$}
Define $x_{\hat{\omega}^{[t]}}$ { $x_{\hat{\omega}^{[t]}}$: *decision variables corresponding to scenario* $\hat{\omega}$ *from time 1 to t*}
Define $\bar{Z}^{[t]}(x_{\hat{\omega}})$ {$\bar{Z}^{[t]}(x_{\hat{\omega}})$: *objective value portion of the original problem for scenario* $\hat{\omega}$ *from time 1 to t*}
for $t \in [1, T]$ **do**
  while $\Phi_{\omega^{[t]}}^{+[t]}$ is not $\emptyset$ **do**
    select scenario $\hat{\omega}^{[t]} \in \Phi_{\omega^{[t]}}^{+[t]}$
    add cut: $Z_{\omega^{[t]}}^{[t]} \geq \bar{Z}^{[t]}(x_{\hat{\omega}^{[t]}})$
  end while
end for

6. Computational experiments

In this section, we present results from our implementation of scenario dominance cuts for solving the case-specific RA-MSS-MIP given in Eqs. (22)-(44). We apply the model to sets of data generated for the state of New Jersey.

6.1. Implementation details

We implement each of the models (cpx, sdc, and ssdc) defined above. All of these models are solved using CPLEX v12.7.1 with default settings, and their respective cuts are added as user cuts. We observe results and compare the three models, cpx, sdc, and ssdc, based on solution time, the optimality gap, and the numbers of nodes generated in the branch and bound tree to solve each formulation.

In our multi-stage stochastic problem, uncertainty is observed in the left-hand side parameter $\beta_{k\omega}^{t}$. For T = 5 stages, we have $3^5 = 243$ scenarios. When defining dominance cuts, we also have to consider the probability of each scenario happening. To calculate probabilities, we use the heuristic algorithm developed in Bushaj et al. (2021). Since we have a high number of scenarios, many dominance relations can be defined. In our problem, it is important to define the scenario dominance cuts by considering the surveillance regime. We categorize the surveillance regime into five groups, which are based on how many years we survey during the 5-year period. These categories are defined as: only survey once, survey twice, survey three times, survey four times, and survey every year. The scenario dominance relations are defined by comparing scenarios within these five categories. For each category, we solve the dominating scenario problem, which will provide the best solution among that category, thus in total, we solve five dominating scenario problems. Due to the large number of cuts that can be generated using scenario relations, we randomly select five dominated scenarios from each category. Therefore, in total, we define 25 sdc cuts for the scenario dominance problem, which makes nearly 10% of the total number of scenarios. Regarding the strong dominance cuts, we solve only one dominating scenario problem, but we solve it for each $t = 1, \ldots, 5$. The number of strong dominance cuts that can be generated increases as we also consider the time dimension.

Computational experiments were conducted in a Workstation with an 8-core Intel CPU reaching 3.6 GHz and 64 GB RAM running a Windows 10 Enterprise and using CPLEX. We use a time limit of 12,000 CPU seconds for solving each test instance.

Table 1
Experiment results for cpx, sdc, and ssdc under different infestation patterns.

(II,DR)	Exp	Cut	Ctime	Time	$\mathbf{T_{imp}}$**%**	Node	Obj	InitGap %	GapImp %
(s,s)	**cpx**	0	0	108	-	0	2,150,592	0.53	-
	sdc	25	8.8	71	34	0	2,150,592	0.43	18.7
	ssdc	502	6.8	55	49	0	2,150,592	0.34	36.2
(s,m)	**cpx**	0	0	113	-	0	1,192,578	0.78	-
	sdc	25	8.8	76	33	0	1,192,578	0.56	28.7
	ssdc	502	7	65	42	0	1,192,578	0.45	42.1
(s,f)	**cpx**	0	0	297	-	0	265,106	0.96	-
	sdc	25	8.8	230	23	0	265,106	0.8	16.9
	ssdc	502	7.8	168	43	0	265,106	0.76	20.6
(l,s)	**cpx**	0	0	108	-	0	420,554	0.61	-
	sdc	25	8.8	80	26	0	420,554	0.57	7.5
	ssdc	502	8	75	31	0	420,554	0.52	14.9
(l,m)	**cpx**	0	0	615	-	829	196,572	0.97	-
	sdc	25	8.8	326	47	169	196,576	0.79	18.4
	ssdc	502	8.2	350	43	374	196,576	0.83	13.7
(l,f)	**cpx**	0	0	702	-	1019	-490,969	0.81	-
	sdc	25	8.8	445	37	657	-490,969	0.6	26.3
	ssdc	502	8.2	483	31	556	-490,969	0.58	29
Overall Average	**cpx**	0	0	324	-	308	622,405	0.78	-
	sdc	25	8.8	205	37	138	622,406	0.62	19.8
	ssdc	502	7.7	199	39	155	622,406	0.58	25.2

6.2. Instance generation and test data

We apply our risk-averse model to the case of EAB management in the state of New Jersey. We describe the economic and EAB-related biological and economic data as well as the generation of test instances for the state of New Jersey in the Online Supplement Section S3 and present the results of the computations in the next section.

6.3. Results

We solve the data sets generated by using different optimization models with specific features defined as below:

- - **cpx**: solving the problem CPLEX 12.7.1 on default settings
- - **sdc**: solving the problem with scenario dominance cuts (70), which are adapted to our case-study problem (22) – (44) as described in Remark 6.
- - **ssdc**: solving the problem with strong scenario dominance cuts (71), which are adapted to our case-study problem (22) – (44) as described in Remark 7.

To report computational results, we define the following columns:

- **T**: number of stages;
- **Sce**: number of scenarios;
- **II**: Initial infestation size of the area [small (s) at 1% or large (l) at 2.5% infestation of the total ash trees];
- **DR**: Infestation dispersal rate [slow (s), medium (m), fast (f)];
- **Exp**: Solution approach (cpx, sdc, ssdc) used;
- **Cut**: Number of inequalities added as user cuts;
- **Ctime**: CPU time in seconds required to solve the scenario subproblems and generate scenario dominance cuts (sdc and ssdc);
- **Time**: CPU time in seconds required to solve the problem, including Ctime;
- $\mathbf{T_{imp}}$: Percentage solution time improvement by cuts over cpx where $T_{imp} = \frac{Time(cpx)-Time(sdc)}{Time(cpx)} \times 100$;
- **Node**: Number of nodes explored in the branch and bound tree;
- **Obj**: Best objective value;
- **InitGap**: Percentage integrality gap of formulation before inequalities are added ($InitGap = 100 \times (Obj - relaxObj)/Obj$), where *relaxObj* and *Obj* are objective function values of the initial LP relaxation and the best feasible solution by cpx, respectively;
- **GapImp**: Percentage improvement in the integrality gap at the root node ($GapImp = 100 \times (1 - rootObj/relaxObj)$, where *rootObj* is the objective function value of the LP relaxation after cuts are added at the root node.

6.3.1. Computational results for scenario dominance cuts

In this subsection, we present results regarding the efficiency of sdc and ssdc on six different test files run for five different budget levels as described in Section 6.2. Each of these 30 instance combinations is run five times for sdc and ssdc in order to capture the randomness in dominated scenario selection to generate the cuts. Thus, we average over five runs for cpx and 25 runs for sdc and ssdc for each test file, as shown in each row of Table 1. This will give an average solution time, which also captures the performance of each model under various budget levels. The Overall Average row gives the results for an overall average of 30 instances. In Table 1, the first column noted as (II, DR) identifies the instance by the characteristics it was created. For example, (s,f) stands for the instances generated using a small initial infestation and a fast infestation dispersal rate.

For all instances, we can see that sdc and ssdc cuts reduce the solution time. In addition, they also reduce the number of nodes in the branch and bound tree. As all our instances have five stages, the complexity of the instances increases as the initial infestation is increased, as the infestation spread rate increases, and as the budget tightens. Interestingly, the cut generation time does not increase much as the complexity of the instance increases.

As the overall average shows in Table 1, sdc cuts improve the solution time by 37% while ssdc improves even more, by 39%. On average, the cpx solution time is 324 CPU seconds, while the time consumed to generate the sdc and ssdc cuts is 8.8 and 7.7 CPU seconds, respectively. By adding cut generation time to the solution time, sdc and ssdc add up to a total solution time of 205 and 199 CPU seconds, respectively. Furthermore, this improvement is achieved without any loss in the optimal solution. In addition, sdc and ssdc help to improve the solution of the problem's linear programming (LP) relaxation, and thus providing a better initial gap compared to cpx, as shown in the **InitGap** and **GapImp** columns. We refer the reader to Table S2 in the supplementary material in Section S4 for more information on the LP relaxation solution and the gap improvement with and without sdc and ssdc with respect to cpx.

Table 2
Experiment results for cpx, sdc, and ssdc under different landscape sizes.

(Size)	Exp	Cut	Ctime	Time	$\mathbf{T}_{imp}$**%**	Binary Variables	Cont Variables	Constraints
5x5	**cpx**	0	0	112	-	91,125	549,180	1,200,020
	sdc	50	8.8	90	20	91,125	549,666	1,200,731
	ssdc	716	8	82	27	91,125	551,367	1,202,496
6x6[a]	**cpx**	0	0	369	-	131,220	789,750	1,726,799
	sdc	50	24	270	27	131,220	790,236	1,727,510
	ssdc	716	18	230	38	131,220	791,937	1,729,2755
7x7[a]	**cpx**	0	0	503	-	178,605	1,074,060	2,349,356
	sdc	50	66	270	46	178,605	1,074,546	2,350,067
	ssdc	716	61	245	51	178,605	1,076,247	2,351,832
8x8[a]	**cpx**	0	0	1,713	-	233,280	1,402,110	3,067,691
	sdc	50	89	883	48	233,280	1,402,596	3,068,402
	ssdc	716	75	720	58	233,280	1,404,297	3,070,167
9x9[a]	**cpx**	0	0	2,860	-	295,245	1,773,900	3,881,804
	sdc	50	92	1,772	38	295,245	1,774,386	3,882,515
	ssdc	716	85	1,623	43	295,245	1,776,087	3,884,280
10x10[a]	**cpx**	0	0	5,210	-	364,500	2,189,430	4,791,695
	sdc	50	115	1,992	62	364,500	2,189,916	4,792,406
	ssdc	716	98	1,719	67	364,500	2,191,617	4,794,171
Overall Average	**cpx**	0	0	1,794.5	-	215,662	1,296,405	2,836,228
	sdc	50	65.8	880	51	215,662	1,296,891	2,836,939
	ssdc	716	57.5	769.8	57	215,662	1,298,592	2,838,704

[a] The data used in this test are simulated data, as described in Section 6.3.1.

Table 3
Comparison of objective values, expected benefit and risk, and costs for the Risk-Neutral, Low, Moderate, and High Risk-Averse models.

	Risk-neutral	Low Risk (α=0.05, λ=10)	Moderate Risk (α=0.25, λ=100)	High Risk (α=0.5, λ=1000)
Objective Value[a]	1,310,000	1,406,286	2,517,570	16,507,780
Exp. Benefit ($)	1,310,000	1,309,930	1,309,290	1,301,480
Exp. Risk ($)[b]	-	9,635	12,082	15,206
Exp. Net Benefit ($)	1,121,280	1,121,230	1,121,170	1,120,710
Exp. Treatment Cost ($)	8,956	8,920	8,773	8,632
Exp. Removal Cost ($)	87,045	87,082	87,230	87,373
Benefit of Scenario H-H-H-H-H ($)	965,810	965,863	965,978	970,124

[a] The calculation with units is represented as Expected Benefit ($) + λ * Expected Risk ($)
[b] The expected risk does not include preceding λ coefficient

To investigate the effect of dominance cuts on larger instances, we generate five more test files by increasing the size of the landscape of the base case of 5-by-5, from 6-by-6 (6x6) to 10-by-10 (10x10), each representing a larger landscape than the base case of 5-by-5 test file. For all the larger landscape generations, we use the same initial infestation size (l) and infestation dispersal rate (s). For each unit increase in the landscape size, we increase a unit budget of 5x5 landscape with (l,s), $200,000. For example, for a 6x6 landscape, we have twice the budget of 5x5, for 7x7, we have three times the budget of 5x5, and thus we end up with a six times larger budget than that of 5x5 in the case of a 10x10 landscape.

Table 2 presents results for cpx, sdc and ssdc for larger instances compared to Table 1. We have used the same cut generation schema as in Table 1, and to account for the change in difficulty, we increase the cut number for **sdc** and **ssdc** models. The tables demonstrate the advantage of the sdc and ssdc cuts over the standard CPLEX solution for larger instances. For example, when all instances are averaged, the solution time improvement due to **sdc** and **ssdc** is 51% and 57%, respectively. Overall, the performance of both sdc and ssdc shows an increasing trend as the instances get larger and harder.

To study the impact of the risk parameters in the time complexity of the model, we perform experiments on a combination of $\alpha = \{0.05, 0.25, 0.5\}$ and $\lambda = \{0.001, 0.1, 1, 10, 1000\}$ values. Computational results show that the sdc and ssdc cuts still improve on risk-averse models for various values of the risk parameters with a similar solution time as the risk-neutral model. For detailed results, see the Online Supplement Section S5.

6.3.2. Comparison of risk-neutral and risk-averse policies

We compare the risk-neutral ($\lambda = 0$) model results with three different risk-averse problems. We set $\lambda = 10$ and $\alpha = 0.05$ to represent low risk aversion, $\lambda = 100$ and $\alpha = 0.25$ to represent moderate risk aversion, and $\lambda = 1000$ and $\alpha = 0.5$ to represent high risk aversion (Table 3).

The optimal objective function values of the risk-averse models are higher than the risk-neutral models because the additional values of risk are added to the objective formulation. When we decompose the objective function into the *expected benefit* $[\mathbb{E}(f(x,\omega))]$ and the *expected risk* $[\lambda CVaR_{\alpha}^{-}(f(x,\omega))]$ in objective function (14), we notice that there is a price for being risk-averse – the expected benefit decreases as we increase the risk aversion (α and λ). In addition, as we become more risk-averse a larger subset of risky scenarios are considered, and the expected CVaR value increases. In other words, the VaR value will get smaller, and the expected positive difference between the VaR and the benefits from risky scenarios will get bigger when considering a higher number of risky scenarios. In Table 3, the *Objective Value* represents the result of the whole multi-objective formulation shown in objective function (22). We also decompose objective function (22) into two parts as in formulation (14): *Expected Benefit* and *Expected Risk*. The Expected Net Benefit is calculated by reducing the expected total management cost from the expected benefit.

We notice that, as we become more risk-averse, the *Objective Value* increases because of the increase in the*Expected Risk* amplified by the λ coefficient. Decomposing the *Objective Value* into two parts shows that as we are more risk-averse, the *Expected Benefit*

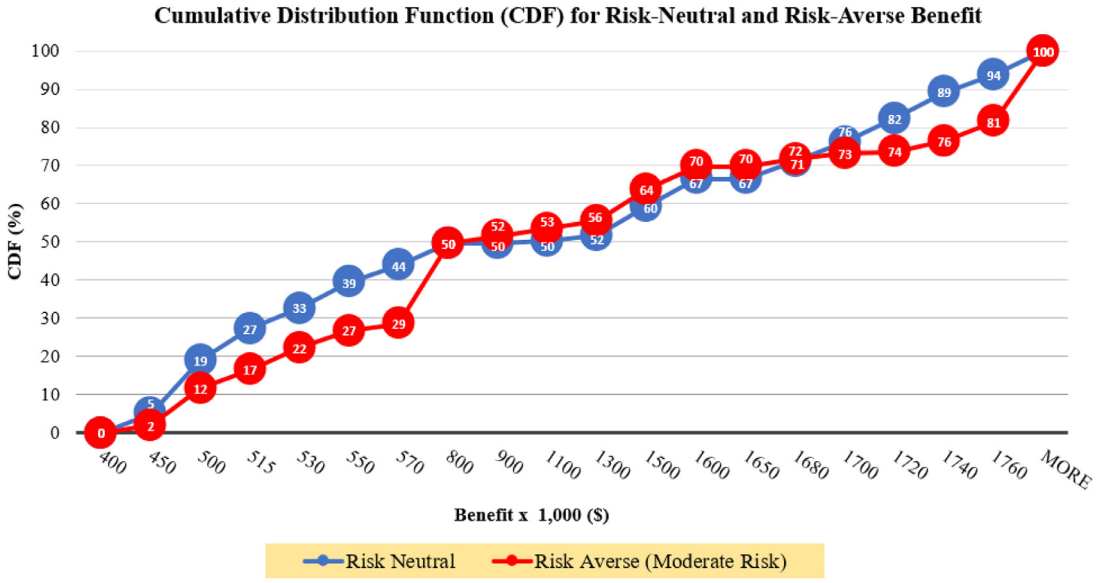

Fig. 1. The CDF of benefit values of all scenarios for risk-neutral and risk-averse models.

decreases, indicating that there is a cost of being risk-averse. The *Expected Net Benefit* decreases, as well. We will analyze the changes in *Expected Net Benefits* with varying risk parameters in more detail in Section 6.3.3. *Expected Treatment* and *Expected Removal* costs, as shown in Table 3, help us understand how the optimal decisions change as the manager becomes more risk-averse. The changes in the optimal costs for both treatment and removal under scenario 0, as we become more risk-averse are shown in Table 3. Here, we notice a shift in budget allocation between treatment and removal decisions as risk-aversion increases; more of the budget is allocated to removing trees rather than treating trees.

With risk neutrality, the treatment of the asymptomatic infested trees at the earliest stage of infestation provides a higher net benefit than removing those trees or no treatment (Bushaj et al., 2021). With risk aversion, the removal of asymptomatic trees is a better option than treatment for the worst-case scenarios. For example, for scenario 0, which involves a high infestation each year, the optimal strategy in the risk-neutral model is to treat as many infested trees as possible each period within the budget. In the risk-averse model, however, a higher benefit is achieved for this scenario by removing these infested trees rather than treating them. Since this scenario has more weight in the risk-averse objective function, the strategy of removing trees rather than treating them increases both the expected benefit and the expected risk portion of the objective function for scenario 0. Further, as the risk aversion increases, the expected treatment cost decreases, and the expected removal cost increases (Table 3).

Similar to the benefit case discussed above, the adjustment of the worst-case scenarios under risk aversion also might affect the full objective, expected benefit, and expected net benefit values of other good-performing scenarios.

Figure 1 compares the cumulative distribution function of the benefit values for each scenario for the risk neutral and moderate risk-averse models. The risk-averse model now tries to find a better budget allocation strategy between treatment and removal to improve unwanted risky scenarios, even if this improvement can cause a decrease in the expected net benefit value. This is also supported by the shift of the low net benefit values towards higher values (see objectives from 450k to 800k) and the fall in the frequency distribution of the high net benefit values (see objective values from 1,720k to 1,760k) under the moderate risk-averse model compared to its risk-neutral counterpart. We notice that the improvement in low benefit values is obtained to increase the overall expected benefit while we can see the fall of the high net benefit values as the price to pay for being risk-averse.

6.3.3. Effect of risk parameters in net benefits

To illustrate further the advantage of using risk measures in our model, we generate some "extreme" scenarios and analyze the *Expected Net Benefit*, the *Expected Profit* over the $100 \times \alpha\%$ worst-case scenarios, and the CVaR under both risk-neutral and risk-averse models. Here, we compute the CVaR of a risk-neutral model by calculating the expected profit over the top $100 \times \alpha\%$ worst-case scenarios. The "extreme" scenarios are generated by changing the realization of infestation for high and low cases. For the high realization, we increase the severity of the infestation from 40% to 80% more than the manager's expectation, while for the low realization, we decrease the severity from 20% to 40% less than the expectation. We validate the impact of risk in our model by performing experiments with α values of 0.05, 0.1, and 0.2 and for each $\lambda \in \{0, 0.1, 0.5, 1, 5, 10, 50, 100\}$.

To investigate further how objective values change under the worst-case scenarios, we plot the expected profit for the top $100 \times \alpha\%$ worst-case scenarios when scenario profit values are sorted in ascending order under both risk-neutral ($\lambda = 0$) and the risk-averse cases ($\lambda > 0$). Figure 2 shows how the least-benefit scenarios are improved using the CVaR risk measure. Notice that for each of the combinations of the risk parameters α and λ, the expected profit over the top $100 \times \alpha\%$ worst-case scenarios under the risk-neutral case ($\lambda = 0$) is improved. The lower the α, the higher the expected profit over the top $100 \times \alpha\%$ worst-case scenarios and the corresponding expected profit is increasing as we increase the λ value. A lower α implies that we are more risk-averse, resulting in a higher expected profit over the worst-case scenarios. That being said, after a certain increase in λ, we do not notice further improvement over the $100 \times \alpha\%$ worst-case scenarios for different α parameters.

6.3.4. Impact of risk-averseness on surveillance frequency

During our experiments, we notice an interesting relationship between the expected risk and the surveillance frequency. In Table 4, we show the risk values for five scenarios having a different surveillance frequency under low, moderate, and high levels of risk aversion. Each scenario is noted using the realization

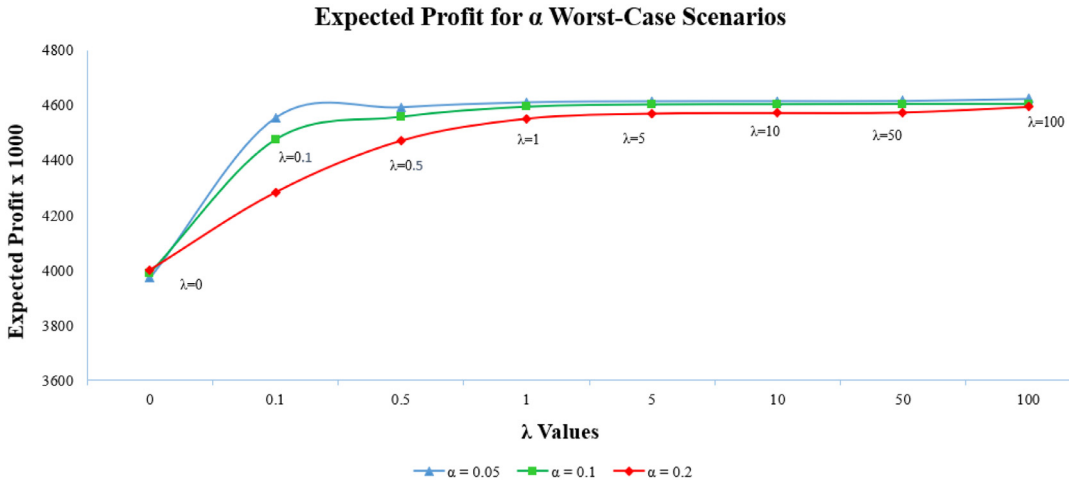

Fig. 2. Expected profit for the top $100 \times \alpha\%$ worst-case scenarios for different values of λ under both risk-neutral ($\lambda = 0$) and the risk-averse cases ($\lambda > 0$).

Table 4
Risk values for five scenario realizations with different surveillance frequency under various risk levels.*

Scenario	Low Risk (α=0.05, λ=10) ($)	Moderate Risk (α=0.25, λ=100) ($)	High Risk (α=0.5, λ=1000) ($)
H-H-H-H-H	4,428	12,260	17,752
M-H-H-H-H	6,755	14,351	20,930
M-M-H-H-H	9,650	21,821	36,621
M-M-M-H-H	15,990	30,354	44,150
M-M-M-M-M	20,432	38,421	58,501

* The risk does not include the λ coefficient

Table 5
Comparison of objective values, expected benefit and risk, and costs for the Risk-Neutral, Low, Moderate, and High Risk-Averse models.

	Risk-neutral	Low Risk (α=0.05, λ=10)	Moderate Risk (α=0.25, λ=100)	High Risk (α=0.5, λ=1000)
Objective Value[a]	1,627,967	5,059,190	8,525,780	12,153,700
Exp. Benefit ($)	1,627,967	1,586,430	1,496,830	1,485,580
Exp. Risk ($)[b]	-	3,171,230	3,175,990	3,206,590
Exp. Treatment Cost ($)	7,248.5	7,236.8.2	7,222.3	7,204.8
Exp. Removal Cost ($)	318,691	329,367	329,624	332,310

[a] The calculation with units is represented as Expected Net Benefit ($) + λ* Expected Risk ($)
[b] The expected risk does not include preceding λ coefficient

for each time stage. As described in Section 5.3, *H* and *L* stand for incurring a high and low realization, respectively, while *M* stands for no surveillance; hence no action is taken in that time stage. For example, the scenario *H-H-H-H-H* represents surveillance at each period of a 5-stage problem and observing a high outcome at each stage. On the other hand, the scenario *M-H-H-H-H* corresponds to no surveillance in the first stage and thus assuming a medium infestation and doing nothing followed by surveillance in stages two to five and observing a high realization. As can be seen from Table 4, as we survey less, the risk increases under each risk-averseness level. This is because as we survey less, we know less about the infestation and make fewer management interventions.

6.3.5. Budget constraint effect on risk mitigation measures

To observe the results without the effect of the budget constraint in the risk mitigation, we modify the original model [(22)–(44)] by adding the left-hand side of the budget constraint (40) as a negative cost in the objective function (22), thus excluding the budget constraint from the model, as shown below:

$$Max \sum_{\omega\in\Omega} p_\omega \left(\sum_{t\in\mathcal{T}} \left(\delta_t \sum_{i\in\Gamma} \left(\zeta S^t_{i\omega} - \sum_{k=1}^{n} \vartheta_k I^t_{ik\omega} - c_1 H^t_{i\omega} - c_2 \sum_{k=1}^{n-2} V^t_{ik\omega} - c_3 \sum_{k=1}^{n} R^t_{ik\omega} \right) \right) + \lambda \sum_{t=2}^{T} \left(\eta^t_\omega - \frac{1}{\alpha} v^t_\omega \right) \right) \quad (77)$$

In this modified model, we also update the risk constraint (23) to include the cost of surveillance, treatment, and removal as shown in the below constraint:

$$v^t_\omega \geq \eta^t_\omega - \delta_t \sum_{i\in\Gamma} \left(\zeta S^t_{i\omega} - \sum_{k=1}^{n} \vartheta_k I^t_{ik\omega} - c_1 H^t_{i\omega} + c_2 \sum_{k=1}^{n-2} V^t_{ik\omega} + c_3 \sum_{k=1}^{n} R^t_{ik\omega} \right)$$
$$\forall \quad t = 2, \ldots, T, \ \omega \in \Omega \quad (78)$$

The modified model without the budget constraint is obtained by replacing Eqs. (22) and (23) with Eqs. (77) and (78), respectively, dropping the budget constraint (40) and keeping all other constraints in the original model the same. Table 5 presents objective values, expected benefit and risk, and expected costs for varying risk-averseness levels for the modified model without the budget constraint. Similar to the results of the original model shown in Table 3, the expected benefit reduces and the expected risk increases as we become more risk-averse. We also observe the same decision shift between treatment and removal costs. As we become more risk-averse, the budget used on treatment decreases while more budget is allocated to the removal actions. Different from the original model with the budget constraint, we notice that a higher amount of money is used for the removal of ash trees. This shows that the budget constraint on the model, apart from the cost of actions we can take, does not affect the trends in the risk-averse decision strategies.

7. Concluding remarks

In this paper, we developed a risk-averse, multi-stage, stochastic mixed-integer programming model where we incorporate a CVaR risk measure into the objective function to control low-objective scenarios. To facilitate an optimal solution to this complex problem, we defined the scenario dominance sets and generated multiple scenario dominance cuts. We applied the RA-MSS-MIP to the problem of designing surveillance and control strategies for emerald ash borer, a non-native forest insect that damages forests in the eastern U.S. In our application, we tested our dominance cuts and strong dominance cuts and compared solution results to the CPLEX solution in default settings. We also examine how the budget allocation policies change from risk-neutral to risk-averse formulations.

Our results show that our implementation of sdc and ssdc cuts reduces the solution time of risk-averse models by CPLEX by more than 30%. Also, we provide results to show that the performance of the sdc and ssdc cuts does not change much with respect to the variations in risk parameters.

By comparing the risk-neutral and risk-averse policies, we show that there is a price for being prepared for the worst-case scenarios. Despite this price, the manager may see this loss as a worthy sacrifice towards the mitigation of possible disaster scenarios. Our results also imply that as the risk-aversion increases, the budget allocation shifts from inexpensive insecticide treatment to more costly tree removal to slow the infestation. This shift in resources happens because tree removal is more effective at slowing the spread of EAB in scenarios with relatively high rates of spread and damage, and these scenarios are given added weight in the risk-averse management objective. Investigating the effects of risk parameter values on the expected net benefits, we show that the number of poor scenarios included in CVaR measure of risk should be decided carefully by adjusting the (α) parameter.

Here, we study a scenario-based formulation of our multi-stage stochastic MIP problem with ECVaR risk measures. The benefit of the multi-stage formulation is that we can capture the spatial-dynamic features of EAB and its host population of ash trees. Further, the model can address questions of the optimal timing of surveillance and subsequent management decisions under a budget designated for multiple periods larger than two stages. The drawback of the multi-stage formulation is that it cannot handle spatial representation of the survey decision because this would explode the scenario tree. A future study could use a two-stage stochastic programming model to analyze decisions on where to survey in the first stage and subsequent management actions in the second stage. But such a two-stage model sacrifices the ability to analyze the optimal sequence of surveys and account for the spatial dynamics of the pest and its host population.

The uncertainty in our case-study model is exogenous, which is also known as decision-dependent uncertainty because the realization of the uncertain infestation depends on the binary surveillance actions that are integrated into a multi-stage scenario tree (Kıbış et al., 2020). A future extension of this work could explicitly use surveillance actions in the mathematical formulation and tackle the complexity of the resulting non-linear mixed-integer program. Another future direction of this study could compare the computational performance of our scenario-based RA-MSS-MIP formulation with a node-based multi-stage formulation using Expected Conditional Stochastic Dominance (ECSD) risk measures.

Future research directions include the development of new ways to decide on the selection of cuts for sdc and ssdc. In our problem, we average over a random selection on the dominance sets, but more research could be done to provide insights on which scenarios can perform better when used to derive cuts.

Another possible future direction can be the introduction of a long-distance dispersal mechanism in addition to the 4-km dispersal algorithm. This method could simulate a long dispersal spread of EAB. Finally, we notice from our results that deciding on the values of (α) and (λ) may provide different insights. More work can be done to provide more assistance to the manager by also providing a recommended risk level for the model solved based on the expectations of the management team.

Acknowledgments

We gratefully acknowledge the support of the U.S. Department of Agriculture, Forest Service, Northern Research Station Joint Venture Agreement No. 16-JV-11242309-109, and the National Science Foundation CAREER Award co-funded by the CBET/ENG Environmental Sustainability program and the Division of Mathematical Sciences in MPS/NSF under Grant No. CBET-1554018.

Supplementary material

Supplementary material associated with this article can be found, in the online version, at doi:10.1016/j.ejor.2021.08.035.

References

Abdelaziz, F. B., Aouni, B., & El Fayedh, R. (2007). Multi-objective stochastic programming for portfolio selection. *European Journal of Operational Research, 177*(3), 1811–1823.

Acerbi, C., & Tasche, D. (2002). Expected shortfall: a natural coherent alternative to value at risk. *Economic Notes, 31*(2), 379–388.

Ahmed, S. (2006). Convexity and decomposition of mean-risk stochastic programs. *Mathematical Programming, 106*(3), 433–446.

Albers, H. J., Fischer, C., & Sanchirico, J. N. (2010). Invasive species management in a spatially heterogeneous world: Effects of uniform policies. *Resource and Energy Economics, 32*(4), 483–499.

Alem, D., & Morabito, R. (2013). Risk-averse two-stage stochastic programs in furniture plants. *OR Spectrum, 35*. https://doi.org/10.1007/s00291-012-0312-5.

Alonso-Ayuso, A., Escudero, L. F., Guignard, M., & Weintraub, A. (2018). Risk management for forestry planning under uncertainty in demand and prices. *European Journal of Operational Research, 267*(3), 1051–1074.

Artzner, P., Delbaen, F., Eber, J., & Heath, D. (1997). Thinking coherently. Risk, 10. *November, 68, 71*.

Aukema, J. E., Leung, B., Kovacs, K., Chivers, C., Britton, K. O., Englin, J., … Liebhold, A. M., et al. (2011). Economic impacts of non-native forest insects in the continental united states. *PLoS One, 6*(9).

Billionnet, A. (2013). Mathematical optimization ideas for biodiversity conservation. *European Journal of Operational Research, 231*(3), 514–534.

Birge, J. R., & Louveaux, F. (2011). *Introduction to stochastic programming*. Springer Science & Business Media.

Bushaj, S., Büyüktahtakın, İ. E., Yemshanov, D., & Haight, R. G. (2021). Optimizing surveillance and management of emerald ash borer in urban environments. *Natural Resource Modeling, 34*(1), e12267.

Büyüktahtakın, İ. E. (2021). Stage-*t* scenario dominance for risk-averse multi-stage stochastic mixed-integer programs. *Annals of Operations Research*, 1–36.

Büyüktahtakın, İ. E., des Bordes, E., & Kıbış, E. Y. (2018). A new epidemics–logistics model: Insights into controlling the Ebola virus disease in West Africa. *European Journal of Operational Research, 265*(3), 1046–1063.

Büyüktahtakin, İ. E., Feng, Z., Frisvold, G., & Szidarovszky, F. (2013). Invasive species control based on a cooperative game,.

Büyüktahtakın, İ. E., Feng, Z., Frisvold, G., Szidarovszky, F., & Olsson, A. (2011). A dynamic model of controlling invasive species. *Computers & Mathematics with Applications, 62*(9), 3326–3333.

Büyüktahtakın, İ. E., & Haight, R. G. (2018). A review of operations research models in invasive species management: state of the art, challenges, and future directions. *Annals of Operations Research, 271*(2), 357–403.

Escudero, L. F., Garín, M. A., Monge, J. F., & Unzueta, A. (2018a). On preparedness resource allocation planning for natural disaster relief under endogenous uncertainty with time-consistent risk-averse management. *Computers & Operations Research, 98*, 84–102.

Escudero, L. F., Garín, M. A., Monge, J. F., & Unzueta, A. (2020). Some matheuristic algorithms for multistage stochastic optimization models with endogenous uncertainty and risk management. *European Journal of Operational Research, 285*(3), 988–1001.

Escudero, L. F., Garín, M. A., & Unzueta, A. (2017). Scenario cluster Lagrangean decomposition for risk averse in multistage stochastic optimization. *Computers & Operations Research, 85*, 154–171.

Escudero, L. F., Monge, J. F., & Morales, D. R. (2018b). On the time-consistent stochastic dominance risk averse measure for tactical supply chain planning under uncertainty. *Computers & Operations Research, 100*, 270–286.

Eyvindson, K., & Cheng, Z. (2016). Implementing the conditional value at risk approach for even-flow forest management planning. *Canadian Journal of Forest Research, 46*(5), 637–644.
Gollmer, R., Gotzes, U., & Schultz, R. (2011). A note on second-order stochastic dominance constraints induced by mixed-integer linear recourse. *Mathematical Programming, 126*(1), 179–190.
Gollmer, R., Neise, F., & Schultz, R. (2008). Stochastic programs with first-order dominance constraints induced by mixed-integer linear recourse. *SIAM Journal on Optimization, 19*(2), 552–571.
Guo, G., & Ryan, S. (2017). Progressive hedging lower bounds for time consistent risk-averse multistage stochastic mixed-integer programs. *URL https://works. bepress. com/sarah_m_ryan/93*.
Hof, J. (1998). Optimizing spatial and dynamic population-based control strategies for invading forest pests. *Natural Resource Modeling, 11*(3), 197–216.
Holmes, E. E., Lewis, M. A., Banks, J., & Veit, R. (1994). Partial differential equations in ecology: spatial interactions and population dynamics. *Ecology, 75*(1), 17–29.
Homem-de-Mello, T., & Pagnoncelli, B. K. (2016). Risk aversion in multistage stochastic programming: A modeling and algorithmic perspective. *European Journal of Operational Research, 249*, 188–199.
Huffaker, R. G., Bhat, M. G., & Lenhart, S. M. (1992). Optimal trapping strategies for diffusing nuisance-beaver populations. *Natural Resource Modeling, 6*(1), 71–97.
Juliano, S. A., & Philip Lounibos, L. (2005). Ecology of invasive mosquitoes: effects on resident species and on human health. *Ecology Letters, 8*(5), 558–574.
Kıbış, E. Y., & Büyüktahtakın, İ. E. (2017). Optimizing invasive species management: A mixed-integer linear programming approach. *European Journal of Operational Research, 259*(1), 308–321.
Kıbış, E. Y., & Büyüktahtakın, İ. E. (2019). Optimizing multi-modal cancer treatment under 3D spatio-temporal tumor growth. *Mathematical Biosciences, 307*, 53–69.
Kıbış, E. Y., Büyüktahtakın, İ. E., Haight, R. G., Akhundov, N., Knight, K., & Flower, C. (2020). A multi-stage stochastic programming approach to the optimal surveillance and control of emerald ash borer in cities. *INFORMS Journal on Computing*, 1–36.
Kovacs, K. F., Haight, R. G., Mercader, R. J., & McCullough, D. G. (2014). A bioeconomic analysis of an emerald ash borer invasion of an urban forest with multiple jurisdictions. *Resource and Energy Economics, 36*(1), 270–289.
Markowitz, H. (1952). Portfolio selection. *The Journal of Finance, 7*(1), 77–91.
Miller, N., & Ruszczyński, A. (2011). Risk-averse two-stage stochastic linear programming: Modeling and decomposition. *Operations Research, 59*(1), 125–132.
Ogryczak, W., & Ruszczyński, A. (1999). From stochastic dominance to mean-risk models: Semideviations as risk measures. *European Journal of Operational Research, 116*(1), 33–50.
Ogryczak, W., & Ruszczyński, A. (2001). On consistency of stochastic dominance and mean–semideviation models. *Mathematical Programming, 89*(2), 217–232.
Onal, S., Akhundov, N., Büyüktahtakın, İ. E., Smith, J., & Houseman, G. R. (2020). An integrated simulation-optimization framework to optimize search and treatment path for controlling a biological invader. *International Journal of Production Economics, 222*, 107507.
Pagnoncelli, B. K., & Piazza, A. (2017). The optimal harvesting problem under price uncertainty: the risk averse case. *Annals of Operations Research, 258*(2), 479–502.
Pejchar, L., & Mooney, H. A. (2009). Invasive species, ecosystem services and human well-being. *Trends in Ecology & Evolution, 24*(9), 497–504.
Pflug, G. C., & Pichler, A. (2016). Time-inconsistent multistage stochastic programs: Martingale bounds. *European Journal of Operational Research, 249*(1), 155–163.
Philpott, A. B., & De Matos, V. L. (2012). Dynamic sampling algorithms for multi-stage stochastic programs with risk aversion. *European Journal of Operational Research, 218*(2), 470–483.
Rockafellar, R. T., Uryasev, S., et al. (2000). Optimization of conditional value-at-risk. *Journal of Risk, 2*, 21–42.
Rockafellar, R. T., & Wets, R. J.-B. (1991). Scenarios and policy aggregation in optimization under uncertainty. *Mathematics of Operations Research, 16*(1), 119–147.
Ruszczyński, A., & Shapiro, A. (2006). Conditional risk mappings. *Mathematics of Operations Research, 31*(3), 544–561.
Schultz, R., & Tiedemann, S. (2006). Conditional value-at-risk in stochastic programs with mixed-integer recourse. *Mathematical Programming, 105*(2-3), 365–386.
Shapiro, A. (2012). Time consistency of dynamic risk measures. *Operations Research Letters, 40*(6), 436–439.
Shapiro, A., Tekaya, W., da Costa, J. P., & Soares, M. P. (2013). Risk neutral and risk averse stochastic dual dynamic programming method. *European Journal of Operational Research, 224*(2), 375–391.
Soleimani, H., & Govindan, K. (2014). Reverse logistics network design and planning utilizing conditional value at risk. *European Journal of Operational Research, 237*(2), 487–497.
Wets, R. J.-B. (1974). Stochastic programs with fixed recourse: The equivalent deterministic program. *SIAM Review, 16*(3), 309–339.
Wilcove, D. S., Rothstein, D., Dubow, J., Phillips, A., & Losos, E. (1998). Quantifying threats to imperiled species in the united states. *BioScience, 48*(8), 607–615.
Yemshanov, D., Haight, R. G., Koch, F. H., Venette, R. C., Swystun, T., Fournier, R. E., … Turgeon, J. J. (2019). Optimizing surveillance strategies for early detection of invasive alien species. *Ecological Economics, 162*, 87–99.
Yin, X., & Büyüktahtakın, İ. E. (2021a). A multi-stage stochastic programming approach to epidemic resource allocation with equity considerations. *Health Care Management Science*, 1–57.
Yin, X., & Büyüktahtakın, İ. E. (2021b). Risk-averse multi-stage stochastic programming to optimizing vaccine allocation and treatment logistics for effective epidemic response. *IISE Transactions on Healthcare Systems Engineering*, 1–23.
Zhang, W., Rahimian, H., & Bayraksan, G. (2016). Decomposition algorithms for risk-averse multistage stochastic programs with application to water allocation under uncertainty. *INFORMS Journal on Computing, 28*(3), 385–404.